# THE RENAISSANCE OF "WATER-IN-SALT" ELECTROLYTES FOR ENERGY STORAGE DEVICES

**BY**

**ARITSA BUNPHENG**

**A THESIS SUBMITTED IN PARTIAL FULFILLMENT OF THE REQUIREMENTS FOR THE DEGREE OF MASTER OF SCIENCE (ENGINEERING AND TECHNOLOGY)**
**SIRINDHORN INTERNATIONAL INSTITUTE OF TECHNOLOGY**
**THAMMASAT UNIVERSITY**
**ACADEMIC YEAR 2024**

THAMMASAT UNIVERSITY

SIRINDHORN INTERNATIONAL INSTITUTE OF TECHNOLOGY

THESIS

BY

ARITSA BUNPHENG

ENTITLED

THE RENAISSANCE OF "WATER-IN-SALT" ELECTROLYTES FOR ENERGY STORAGE DEVICES

was approved as a partial fulfillment of the requirements for
the degree of Master of Science (Engineering and Technology)

on December 25, 2024

Chairperson

(Assistant Professor Wisit Hirunpinyopas, Ph.D.)

Member and Advisor

(Assistant Professor Pawin Iamprasertkun, Ph.D.)

Member

(Associate Professor Khanin Nueangnoraj, Ph.D.)

Director

(Professor Pruettha Nanakorn, D.Eng.)

| | |
|---|---|
| Thesis Title | THE RENAISSANCE OF “WATER-IN-SALT” ELECTROLYTES FOR ENERGY STORAGE DEVICES |
| Author | Aritsa Bunpheng |
| Degree | Master of Science (Engineering and Technology) |
| Faculty/University | Sirindhorn International Institute of Technology/ Thammasat University |
| Thesis Advisor | Assistant Professor Pawin Iamprasertkun, Ph.D. |
| Academic Years | 2024 |

# ABSTRACT

In recent years, there has been a growing focus on the demand for alternate electrolytes. There is a requirement to tackle the drawbacks of costly alternatives like lithium bis(trifluoromethanesulfonyl)imide (LiTFSI) in energy storage applications. This study explores a range of lithium salts (LiX) as potential substitutes, focusing on their suitability for "water-in-salt" electrolytes. By investigating electrolytes with concentrations varying from low to superconcentrated levels, the physical and electrochemical properties of LiX were thoroughly examined. Parameters such as viscosity, pH, conductivity, density, and temperature variations during mixing were meticulously evaluated to understand the behavior of LiX electrolytes.

Electrochemical characterization using carbon-based materials in a three-electrode configuration and subsequent integration into coin cell supercapacitors provided insights into the performance of different LiX electrolytes. Notably, while highly concentrated LiX electrolytes, particularly LiCl, demonstrated the potential to expand the operating voltage window, challenges related to corrosion were identified, necessitating further mitigation strategies.

Studies have also shown redox properties in LiBr and LiI electrolytes, with increased concentration observed to accelerate the redox process while maintaining

voltage stability. $LiNO_3$ becomes It is a potent alternative electrolyte. This is due to its potential being comparable to LiTFSI and its cost-effectiveness.

Cost analysis shows that $LiNO_3$ is a feasible option in terms of energy density. It has the potential for further optimization through the use of LiBr and LiI as redox enhancing electrolytes. This comprehensive review not only provides valuable insights into the physical and electrochemical characteristics of LiX electrolytes, but also highlights the potential of these electrolytes as alternatives. In the electrolyte system "Water in salt". Overall, this research contributes to improving our understanding of LiX electrolytes and leads to their practical use in next-generation energy storage devices. It offers a promising path towards cost-effective and efficient energy storage solutions.

**Keywords**: Water-in-salt, Electrolyte, Energy storage, Lithium-ion

# ACKNOWLEDGEMENTS

The research work has been conducted in the School of Bio-chemical Engineering and Technology, Sirindhorn International Institute of Technology; SIIT, Thammasat University. First of all, I would like to acknowledge to the postgrad scholarship from Sirindhorn International Institute of Technology, Thammasat University (faculty's quota), for providing me with the scholarship, and Research unit in sustainable electrochemical intelligent (RU-SEI) for providing facilities and resources for research.

Further, I would like to thank my supervisor, Assistant Professor. Dr. Pawin Iamprasertkun for giving me this opportunity to study and for all the valuable advice, motivation, and encouragement. Without continuous help, this thesis would not have been done. I am sincerely thankful to my thesis committee, Associate Professor. Dr. Khanin Nueangnoraj for advice and invaluable expertise during my study. I express special thanks to the Assistant Professor. Dr. Wisit Hirunpinyopas, the committee member (Department of Chemistry and Centre of Excellence for Innovation in Chemistry, Faculty of Science, Kasetsart University) for their kind instruction. These extensive discussions and exploration have been very helpful for my thesis. And Dr. Kanokporn Tangthana-umrung from the National Nanotechnology Center (NANOTEC) for the contact angle measurement.

I am also thankful to the School of Bio-chemical Engineering Technology and all its staff members for their guidance. Finally, I cannot forget to thank my family for all the unconditional support in this very intense academic year.

Aritsa Bunpheng

# TABLE OF CONTENTS

# LIST OF TABLES

# LIST OF FIGURES

# LIST OF SYMBOLS/ABBREVIATIONS

| Symbols/Abbreviations | Terms |
|---|---|
| AC | Activated Carbon |
| ASCs | Asymmetric Supercapacitors |
| CB | Carbon Black |
| CV | Cyclic Voltammetry |
| EDLCs | Electrical Double-Layer Capacitors |
| EES | Electrochemical Energy Storage |
| ESW | Electrochemical Stability Window (ESW) |
| GCD | Galvanostatic Charge-Discharge) |
| IL | Ionic Liquid (IL) |
| LiTFSI | Lithium bis(trifiuoromethane-sulfonyl) imide |
| LiBr | Lithium bromide |
| LiCl | Lithium chloride |
| LiI | Lithium iodide |
| LiNO3 | Lithium nitrate |
| Li2SO4 | Lithium sulfate |
| LIB | Lithium-Ion Battery |
| LICs | Lithium-Ion Capacitors |
| NMP | N-methyl-2-pyrrolidone |
| PVDF | Polyvinylidene Fluoride |
| SCs | Supercapacitors |
| SSCs | Symmetric Supercapacitors |

# CHAPTER 1
# INTRODUCTION

Energy storage materials have received a great deal of attention in the past twenty years. Supercapacitors in particular have emerged as very promising energy storage devices. Especially for flexible electronic devices. Improving the performance and functionality of supercapacitors relies heavily on the development of suitable materials. Supercapacitors have shown superior energy density compared to traditional capacitors and have a higher energy density compared to batteries. There is a great demand for advances in the field of electrochemical supercapacitor cells. A separator that can withstand high temperatures. Flexible supercapacitors and electrolyte solutions with high electrical conductivity Therefore, the electrochemical performance energy density. The charge storage density, specific capacity, and charge/discharge ratio of supercapacitors have finally been improved.

## 1.1 Background

Lithium-ion capacitors (LICs) have been attracted much attention as a next generation of capacitive due to its high energy density compared to conventional electrical double-layer capacitors (EDLCs), and its high-power density compared to batteries as well as having the long cycle life (Cao, Shih, Zheng, & Doung, 2014; Zhang et al., 2019). LICs consists of the negative electrode of high energy density from lithium-ion battery (LIB) and positive electrode of EDLCs from activated carbon (AC) (Cao et al., 2014; Cappetto et al., 2017; Zhang et al., 2019). Enormous researches have been carried out to optimize the electrochemical performances of the LICs involving the selection and tunability of electrode materials, electrolytes and separators (Amatucci, Badway, Du Pasquier, & Zheng, 2001). The selection of components can be the first consideration to minimize the trade-off between the electrode performance and the material cost.

Until now, several type of materials such as metal compound and organic compounds have been produced as the battery-type electrodes in LICs (Deng, Lei, Zhu, Xiao, & Liu, 2018; Zhao, Wang, Cao, Cai, & Sui, 2017). Although they can provide a

high specific capacity and excellent electrochemical properties, the development of LICs is still limited by the low conductivity and wide volume expansion from these materials (Zou et al., 2020). To overcome this drawback, carbon-based electrodes especially activated carbon have been extensively chosen in energy storage system due to their low expense, sufficient supplies and superior physical and chemical stability (Lamb & Burheim, 2021). It was also known that porous carbon-based materials are utilized as anode and cathode which can act in lithium-ion intercalation/deintercalation mechanism and the ions adsorption/desorption behavior, respectively (Lang et al., 2018; L. Wang & Hu, 2018)

Besides electrode design, the efficiency of electrolytes is also needed to improve the energy density of LICs without losing the advantages of a high-power density and a life cycle property. Thus, the reasonable design of electrolytes has become the latest focus to achieve high energy density (Zou et al., 2020). In general, aqueous electrolytes are considered as a safe, non-flammable, and easy to handle, but the ESWs obtained are restricted around 1.23 V owing to water electrolysis. To overcome this issue, Suo et al. (2015) developed water-in-salt electrolytes (WiSEs) where the weight and volume ratios of ionic salt are greater than that of water (Suo et al., 2015). The presence of salt can bind more free water molecules and restart the electrochemical activity of water resulting in an extension of the voltage window. Lithium bis (trifluoromethane sulfonyl) imide (LiTFSI) salt was dissolved in water at extremely high concentrations of 21 m (mol $kg^{-1}$, mol of salt in kg of water). The exhibition of LiTFSI can extend the ESWs greater than 3.0 V by using stainless steel as an electrode (Suo et al., 2015).

From the perspective of lithium-ion capacitance design, it is necessary to produce the prototypes in a fully size of cell, to investigate in the electrochemical performance, energy density, life cycle and safety (Kwade et al., 2018). Before that, the cell chemistry is first optimized in a small scale to examine the cell performance, typically coin cells or an equivalent. Hence, all the parameters including the anode and cathode active materials, film thickness, porosity and particle size, electrolyte concentration, ion conductivity, viscosity and cell design are optimized. Then, the cell could be scaling up to a fully engineered pouch cell based on the optimization algorithms to design a better prototype with certain high electrochemical performance and improve life cycle (Bridgewater et al., 2021). This approach is approved by every

lithium-ion cell manufacturing. Herein, we propose to develop the pouch cell capacitor with the use of a variation of WIS electrolytes. The influent parameters in terms of material designs, electrode designs and cell structures are investigated for the development of electrochemical performance of lithium-ion pouch cell capacitor. The obtaining LICs pouch cells could achieve high ESWs and energy density of ~3 V with more than 13 Wh/kg. This could extend the cycle life of LICs pouch cells.

**1.2 Objectives**

1.2.1 The development of water-in-salt electrolytes (WISE) for energy storage applications, especially supercapacitors (also refer to lithium-ion capacitors). The lithium-ion-based electrolytes such as lithium chloride (LiCl) are investigated at various concentrations from dilute to high (called “water-in-salt”) concentrations (1 to 20 m).

1.2.1 Explore the electrochemical properties of the electrolyte combination to further investigate the possibility of fabricating the “water-in-salt” supercapacitors (also refer to lithium-ion capacitors).

1.2.3 The variety of lithium salt base electrolytes was studied, herein e.g., LiCl, LiBr, LiI, $LiNO_3$, $Li_2SO_4$, and LiTFSI. The electrochemical properties of WISE are studied and optimized for use in lithium-ion pouch cell capacitors.

1.2.4 Demonstrate the preparation procedure of “water-in-salts” in an engineering level: cost, energy consumption, energy utilization, and unit operation.

# CHAPTER 2
# REVIEW OF LITERATURE

## 2.1 Background and Motivation of Supercapacitors (SCs)

Electrochemical energy storage (EES) devices play an important role in the electrical network by securing continuous energy delivery (Soltani & Beheshti, 2021). There consisted of two main systems for reversible electrochemical energy storage including secondary batteries, and supercapacitors (SCs) (Zou et al., 2020). Battery charges through the faradaic Li-ion insertion with high energy density of about 200 Wh/Kg while the power density is limited of less than 2 kW/kg by the kinetic of $Li^+$ diffusion process in electrodes (Zou et al., 2020). On the other hand, SCs also known as electrical double-layer capacitors (EDLCs) provide high power density due to the reversible of ion adsorption and desorption at the interface between electrode material and electrolyte solution. Although SCs have the advantages of high-power density, good durability, and long-life cycle over existing of secondary batteries, they still have drawbacks in terms of energy density and cost production (Jagadale et al., 2019).

Supercapacitors (SCs) function similarly to conventional capacitors but offer significantly greater capacitance and notably improved energy and power density. They are categorized into electrochemical double-layer capacitors (EDLCs), hybrid capacitors, and pseudocapacitors based on their charge storage mechanism (Ramachandran et al., 2023). Based on the electrode material utilized, supercapacitors are categorize into two primary groups: symmetric supercapacitors (SSCs) (Zhao et al., 2020) and asymmetric supercapacitors (ASCs) (Ali, 2020). Symmetric supercapacitor comprises two identical electrodes, whereas an asymmetric supercapacitor utilizes two dissimilar electrodes, with one typically fabricated from porous carbon and the other resembling a battery-type electrode. Despite minor variations in the operational principles of different supercapacitors, the choice of active materials profoundly influences overall device performance. Recent advancements in engineering and materials science have facilitated the development of novel materials exhibiting substantially improved energy and power density characteristics during electrochemical storage. The Ragone plot, as depicted in Figure 2.1, presents a concise comparative

analysis of diverse energy storage devices based on their power and energy densities. Continuously evolving, these plots reflect ongoing advancements in technology. The global proliferation of emerging electronic and optoelectronic technologies accentuates the imperative for more robust power solutions characterized by heightened energy densities and prolonged operational lifespans(Jiang et al., 2021).

Supercapacitors, as a highly promising energy-storage technology, exhibit several advantageous features, including high power density, rapid charge and discharge rates, and extended cyclic stability (Riaz, Sarker, Saad, & Mohamed, 2021; Sajjad, Khan, Cheng, & Lu, 2021) However, the existing supercapacitors suffer from a critical limitation: their extremely low energy density, which significantly constrains their practical applications. To address this challenge, researchers are actively exploring novel supercapacitor designs with enhanced performance Asymmetric supercapacitors (ASCs), constructed using distinct electrode materials, offer a notable advantage of an extended operational voltage window which substantially enhances their energy density

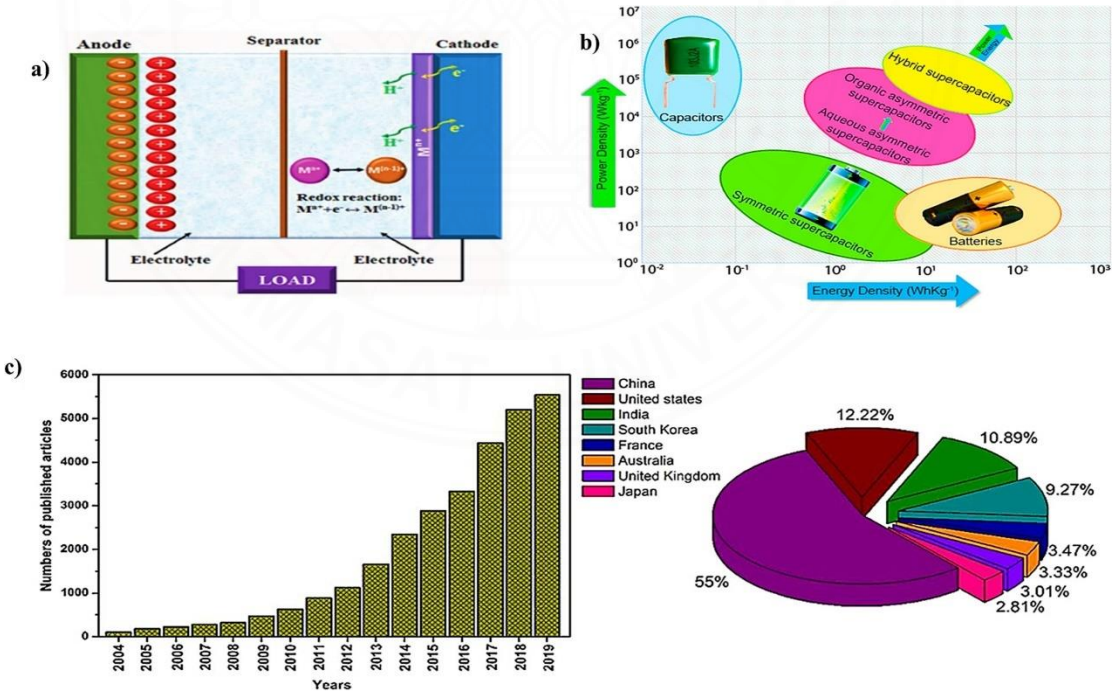


**Figure 2.1** a) An illustration depicting a common configuration of an asymmetric supercapacitor. b) Ragone plot showcasing the energy and power densities of different energy storage devices. c) Research publications focusing on the development and research of asymmetric supercapacitors(Choudhary et al., 2017).

Supercapacitors (SCs), in comparison to batteries, offer significant advantages in energy storage. Notably, SCs exhibit a linear voltage increase during constant current charging, a feature attributed to charge storage within the electrodes. This behavior is evident in Figure 2.2, where the CV (cyclic voltammetry) curve for SCs appears rectangular when the current remains nearly constant during charge-discharge cycles. In contrast, batteries exhibit pronounced peaks indicative of faradaic current. Additionally, when examining GCD (galvanostatic charge-discharge) curves, SCs display a sloped shape, while batteries show a relatively flat curve (Huang, Yuan, & Chen, 2022). Recognizing these benefits, ongoing research aims to enhance SCs' power and energy density

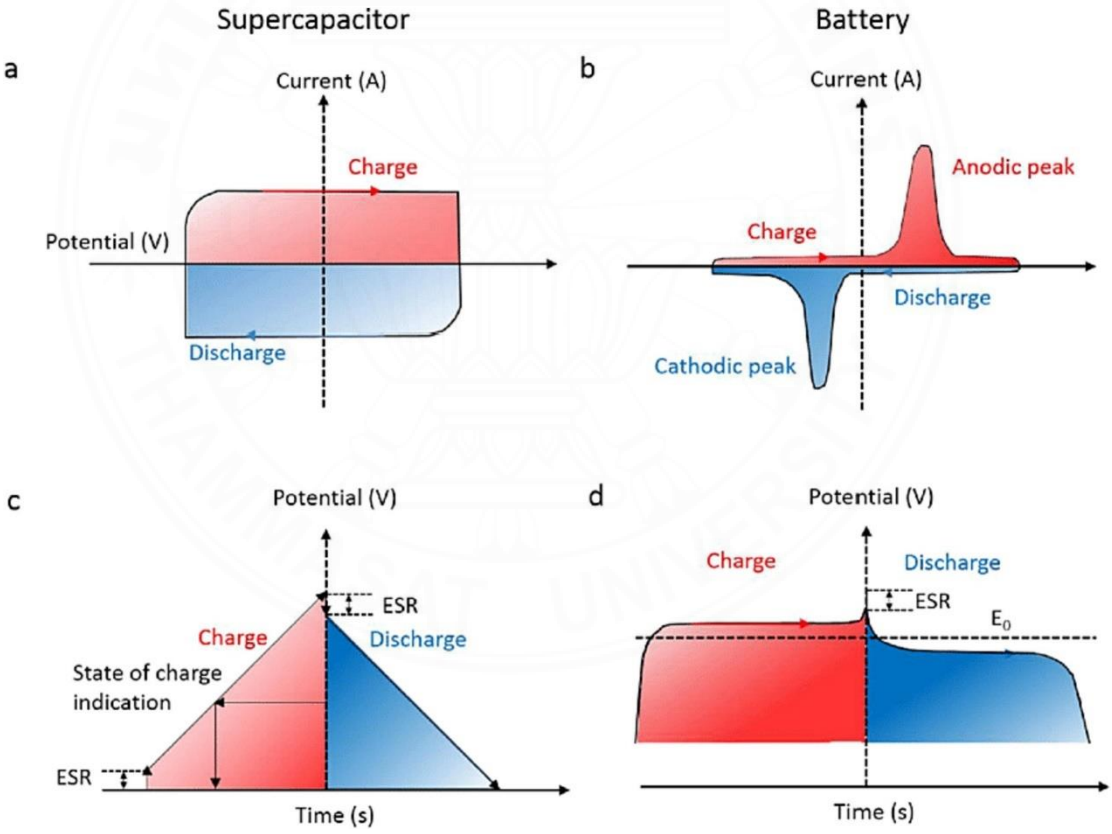


**Figure 2.2** Comparison of the electrochemical characteristics of supercapacitors (SCs) and batteries (Shao et al., 2018).

## 2.2 Fundamentals of supercapacitors

The total energy stored in the EDLC depends on by multiple important factors, such as the capacitance of the active materials and the operating voltage window. In this context, C represents the capacitance, Q refers to the total charge, V represents the voltage, A represents the surface area of the electrode, and d represents the distance between two opposite electrodes. To improve energy densities, there are two possible approaches: either enhance the specific capacitance, which is closely linked to the intrinsic qualities of the material such as its surface area or extend the operating voltage window, which is directly related to the characteristics of the electrolyte. The electrolytes properties have a more significant impact on the energy density. Electrolytes can be categorized into three different groups: (1) aqueous, (2) organic, and (3) ionic liquid (IL) electrolytes (Table 2.1). Aqueous electrolytes have a limited range of voltage where water breaks down when the potential exceeds 1.23 V. On the other hand, IL electrolytes have a wider voltage range, but their low ionic conductivity results in lower power densities. Additionally, IL electrolytes require higher temperatures for effective operation. Additionally, the expensive cost of IL electrolytes is an obstacle to their commercialization.

**Table 2.1** Different categories of electrolytes used in supercapacitors and their corresponding properties (J. M. Lim et al., 2023).

| | **Aqueous** | **Organic** | **Ionic liquid** |
|---|---|---|---|
| Stable potential window (V) | 0.8–2.0 | 2.5–2.8 | 3.5–4.5 |
| Ionic conductivity | High | Middle | Low |
| Cost | Low | Middle | High |
| Manipulability | Simple | Complex | Middle |
| Flammability | None | High | Middle |
| Toxicity | None | High | Low |
| Volatility | Middle | High | Low |
| Chemical/thermal stability | Middle | Low | High |

Therefore, the most commonly available variation that is probably to be utilized in energy storage systems (ESSs) is the EDLC supercapacitors based on organic electrolytes, which offer a limited range of operating voltage.

## 2.3. Electrolyte considerations for supercapacitors of the EDLC type

Electrolytes have a significant impact on the overall performance of supercapacitors (SCs) by increasing their energy densities, expanding their operating voltages, and improving their long-term stability. The physical and chemical properties of electrolytes have an essential part in achieving these enhancements.

Figure 2.3 display a comparative analysis of various significant factors among the three groups of electrolytes (Nguyen, Kim, & Lee, 2021; X Wu, Yang, Yu, Liu, & Li, 2021). The cell voltage is primarily constrained by the electrochemical stability window (ESW) of electrolytes, which is generally accepted. The electrochemical potential window (ESW) of electrolytes, which is the difference between the reduction and oxidation potentials, is affected by the characteristics of ions (including cations and anions), solvent molecules, and the interactions between ions, solvents, and the electrode surface (Pal, Yang, Ramesh, Thangadurai, & Jose, 2019). In order to get high-voltage electrochemical double-layer capacitors (EDLCs) using supercapacitors (SCs), electrolytes that are composed of ionic liquids (ILs) and organic solvents are more commonly employed compared to aqueous electrolytes due to their larger electrochemical stability window (ESW). However, differences in the electrochemical stability windows (ESWs) might occur even when using the same electrolyte, as it is closely related to the unique electrode materials utilized (Ruschhaupt, Pohlmann, Varzi, & Passerini, 2020). The electrochemical window (ESW) of an electrolyte is usually wider on inert electrodes such as platinum and glassy carbon than on porous carbon electrodes. This is because the carbon surface has a higher concentration of functional groups (Nguyen et al., 2021; K. Xu, Ding, & Jow, 2001). Therefore, the amount of purity of electrode materials, the existence of functional groups on the active materials, and the physical stability of the active materials are all important elements that affect the electrolyte's ESW(Pal et al., 2019). Therefore, it is essential to carefully design electrolytes, active materials, and electrode materials in order to create high-voltage EDLCs.

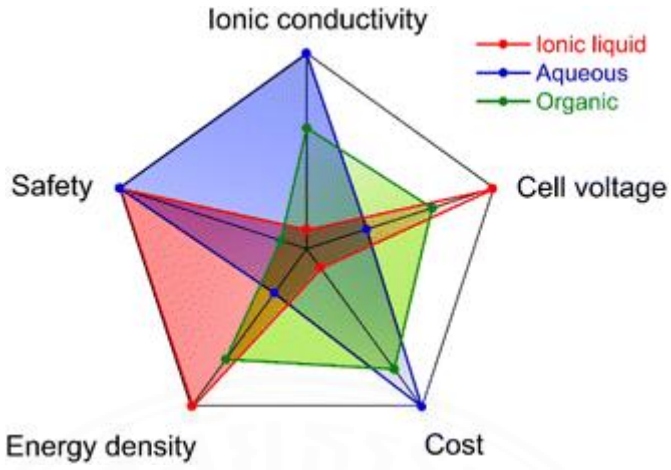


**Figure 2.3** An analysis of the characteristics and efficacy of IL, aqueous, and organic electrolytes(Nguyen et al., 2021).

Researchers have made major advancements in expanding the operating potential range for supercapacitors (SCs) by developing organic electrolytes in the field of electrolyte development. This involves the use of advanced organic solvents that have a wider range of stability for electrochemical reactions, as well as the addition of novel solvents and ion additions into the electrolyte solution. Moreover, the utilization of inorganic additives and the incorporation of a passivation layer on electrode materials have demonstrated efficacy in expanding the range of operating potential and improving the longevity of the electrolyte. Future research on electrolytes will focus on three main areas: firstly, finding a new organic electrolyte that is cost-effective and has a high energy storage capacity (ESW); secondly, investigating a new electrolyte additive that is economical and can increase the ESW of the electrolyte; and thirdly, creating a non-toxic and non-flammable electrolyte with a high ESW. In addition, future research efforts will require the addition of enhanced electrolytes and electrode materials, together with associated optimization efforts, to achieve long-term stability and high voltage in supercapacitors.

## 2.4 Electrolytes

The electrolyte composition and its electrochemical stability window play an important role in the determination of the energy densities of SCs since this parameter is proportional to the square of the voltage. In general, the electrolyte is specifically designed to support a particular use in SCs applications. The electrolytes of SCs are usually classified into three categories: i) organic electrolytes, ii) pure ionic liquid (IL) electrolytes, and iii) aqueous electrolytes (water-in-salts)

### 2.4.1 Organic electrolyte

An organic electrolyte system is mainly composed of the organic solvent such as acetonitrile (ACN) or propylene carbonate (PC) and the ionic electrolytes e.g., tetraethylammonium tetrafluoroborate ($TEABF_4$), lithium perchlorate ($LiClO_4$) and lithium hexafluorophosphate ($LiPF_6$). In addition, organic electrolyte system can be used in quasi-solid state, which is combined with polymer host and organic electrolyte. The major advantage of organic electrolyte exhibit as the wider ESW (2.5-2.8 V) (Zhong et al., 2015). The optimized properties of various organic solvent and electrode materials are extensively studied to provide suitable conditions for SCs. Water should be avoided as much as possible in organic electrolytes because it can reduce the capacitor performance and induce the degeneration of self-discharge (Kurzweil & Chwistek, 2008). However, the drawbacks of organic electrolyte are exposed in terms of flammability and highly cost. In addition, the overcharge of the capacitor can also generate toxic volatile substances, resulting in the loss of power storage capacity (H. Wang & Yoshio, 2010).

### 2.4.2 Ionic (IL) electrolyte

Ionic electrolytes can be synthesized by composing of organic cation with different anions (Armand, Endres, MacFarlane, Ohno, & Scrosati, 2009). Their main interest lies in the large ESW which can be up to 6 V (Brandt, Pohlmann, Varzi, Balducci, & Passerini, 2013). In addition, IL electrolytes have a high thermal stability, wide liquid range, high conductivity and ion mobility, low volatile, and low cost. Nevertheless, SCs with IL electrolyte system contain relatively high viscosity. As a consequence, the IL electrolyte and activated carbon (AC) cannot be well infiltrated.

The power of IL-based SCs system is too low which compared to aqueous-based SCs (Ye, Wang, Ning, Zhong, & Hu, 2021). Since SCs are prominently mentioned as a high-power devices, it is clearly seen that the limited power of IL-based SCs represents a drawback that needs to be improved for the real use in commercial devices (Brandt et al., 2013).

### 2.4.3 Aqueous electrolyte

Investigating aqueous electrolytes as a result of their strong emphasis on battery safety. These electrolytes typically function at voltages below 1.23 V to avoid deterioration. Suo et al. have overcome this restriction by introducing a water-based solution of lithium bis (trifluoromethanesulfonyl) imide, which allows for the production of an electrolyte with an impressive electrochemical range of 3 V. Smith and Dunn's Perspective highlights a significant advancement that involves the use of concentrated solutions to efficiently prevent hydrogen evolution and electrode deterioration. At these concentrations the solvation shell of lithium experiences alterations as a result of the inadequate quantity of water present to counterbalance the Li+ charge. Therefore, this groundbreaking method proposes the possibility of substituting combustible organic electrolytes with a more secure aqueous substitute.

Aqueous electrolytes have been widely investigated for EES devices due to their economical cost, environmental-friendly, high conductivity, and high specific capacitances (Baptista, Sagu, KG, & Lobato, 2019). As opposed to ILs and organic electrolytes, aqueous electrolytes are safe and easily prepared. However, the main disadvantage of aqueous electrolytes is restricted by the decomposition of water at high voltage (~1.2 V), which cause the limitation of ESW as compared to other electrolytes. In addition, the appropriate temperature of aqueous based electrolytes is confined by the water properties (Baptista et al., 2019; Zhong et al., 2015). Table 2.2 provides some information of aqueous-based electrochemical SCs and their properties.

**Table 2.2** Aqueous electrolytes-based SCs and their performance

| Electrode materials | Cathode/anode material | Electrolyte | Cell Voltage (V) | Power Density (W/kg) | Energy density (Wh/kg) | Specific capacitance (F/g) | Ref. |
|---|---|---|---|---|---|---|---|
| Hydrous $RuO_2$ | $RuO_2/RuO_2$ | 1M $Na_2SO_4$ | 1.6 | 500 | 18.77 | 52.66 | (Xia, Shirley Meng, Yuan, Cui, & Lu, 2012) |
| Mesoporous $MnO_2$ | - | 0.65M $K_2SO_4$ | 1 | 70 | 24.1 | 224.88 | (G. R. Li et al., 2010) |
| $NiCo_2S_4$ nanocages | $NiCo_2S_4$ /AC | 3M KOH | 1.6 | 689.5 | 41.4 | 120 | (Liu, Zhang, Li, Liu, & Wang, 2019) |
| Mn-PANI/SWCNT | - | 1M KCl | 1.6 | 550 | ~194.13 | 546 | (Dhibar, Bhattacharya, Hatui, Sahoo, & Das, 2014) |
| Graphene/mPANI | - | 1M $H_2SO_4$ | 0.7 | 106.7 | 11.3 | 749 | (Fan et al., 2017) |

In summary, each type of electrolyte has its own advantages and disadvantages, and it is difficult for a single type of electrolyte to achieve the increasing requirements of SCs.

### 2.4.4 Water in Salt electrolyte

Unlike conventional electrolytes, superconcentrated so-called "water in salt" (WiSE) electrolytes have developed special properties that make them a crucial candidate for new-generation energy storage devices. The key feature that highlights the WiSE properties is the solvation process, which is completely different than in classical water electrolytes. In the WiSE electrolyte system, the weight or volume ratio of salt to water is more than 1 (Chen, Feng, & Qiao, 2020) (Liang, Hou, Dou, Zhang, & Yan, 2021). Therefore, the number of water molecules surrounding the ions is significantly reduced and depends on the salt concentration. As a consequence, the structure of the interfacial region changes; with a properly designed electrolyte, it is possible to greatly reduce the water decomposition. As a result, WiSE exhibited the remarkably enhanced ESWs (Chen et al., 2020).

Several pH-neutral WiSEs such as $Li_2SO_4$, $Na_2SO_4$, and $K_2SO_4$ have been used in electrochemical capacitors (He, Fic, Frackowiak, Novák, & Berg, 2016). However, the solubility of these salts is too low, so they cannot be considered as the previously WiSE concepts. In addition, It is also known that the performance of EC also depends

on ion mobility. Therefore, the introduction of highly conductive neutral electrolytes is essential for high power storage. An example of such salts for aqueous electrolytes can be found in Figure 2.4. The molarity of saturated under standard conditions is determined at $H_2O$ in 25 °C (Galek, Frackowiak, & Fic, 2020).

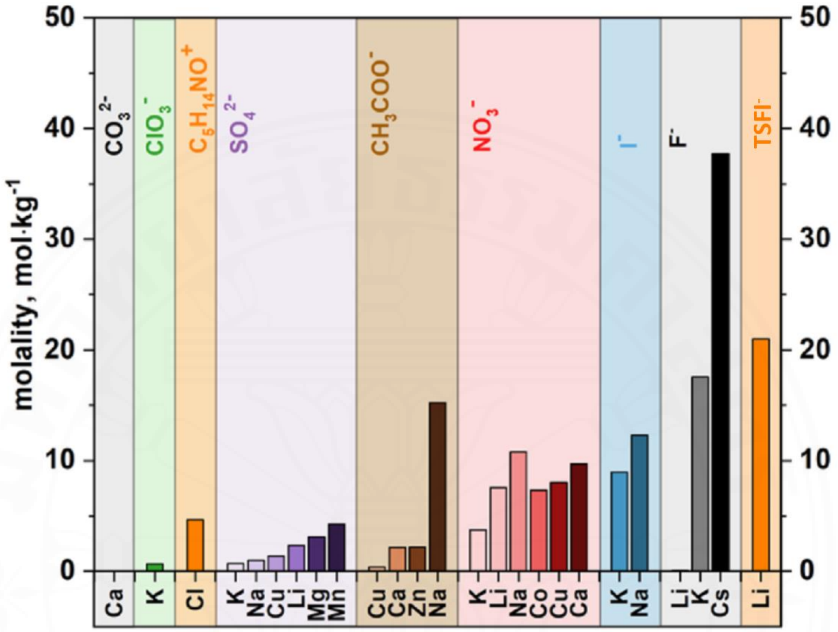


**Figure 2.4** The molality of saturated aqueous solutions of the compounds most often applied in electrolyte formulations (standard conditions).

Lithium bis (trifluoromethane sulfonyl) imide (LiTFSI) salt, Suo et al. (2015) developed water-in-salt electrolytes (WiSE) using high concentration Lithium bis (trifluoromethane sulfonyl) imide (LiTFSI) salt (Suo et al., 2015). In this research, LiTSFI salt was dissolved in water at a extremely high concentrations around 21 m. The exhibition of LiTFSI can extend the ESWs up to 3.0 V which is much higher when comparared to the aqueous electrolyte at normal concentration. The presence of salt can bind more free water molecules and retard the electrochemical activity from water resulting in an extension of the ESW (Suo et al., 2015). Lannelongue et al. (2018) then studied further about the influence that electrolyte molality has on the overall performance of symmetric SCs with activated carbon electrodes and LiTFSI electrolyte (Lannelongue et al., 2018). In this research, a cell voltage of 2.4 V can be applied using the 31.3 m “water-in-LiTFSI” solution whereas it is only 1.2 V in conventional aqueous

devices. Please note that from our experiment found that the maximum electrolyte concentration of the LiTFSI is about 21 m. As a consequence, the specific capacitance of SCs can be improved by using “water-in-salt” electrolytes. The energy density of 30 Wh/kg was obtained which is at least three times greater than for conventional aqueous devices. However, the power density obtained at high concentration (31.3 m) was low but increased as the WiSE concentration decreased (Lannelongue et al., 2018).

Limitation of WISE based on LiTFSI, During the 1990s, Armand et al. presented a comprehensive overview of the development of a novel electrolyte salt known as LiTFSI (Armand, 1991). Subsequently, researchers have explored its exceptional chemical stability and passivation capabilities, leading to the emergence of pioneering research areas such as WISEs (Bouchet et al., 2013; Suo et al., 2015). An inherent challenge with LiTFSI lies in its corrosive nature towards aluminum current collectors, significantly restricting its applicability in current battery systems (Matsumoto et al., 2013). Despite the frequent comparison of LiTFSI WISEs to existing LIB electrolytes (such as $LiPF_6$ in carbonates) and their potential as alternatives (Droguet, Grimaud, Fontaine, & Tarascon, 2020), the production of LiTFSI remains a relatively understudied subject in scientific research. Therefore, gaining insight into the manufacturing process of LiTFSI and its requisite raw components is essential for advancing research and development in this field.

Lithium sulfate ($Li_2SO_4$) salt, Y.Wang et al. (2006) prepared the hybrid supercapacitor by using 1 M Lithium sulfate ($Li_2SO_4$) as an electrolyte. In this case, activate carbon was used as a negative electrode and $LiMn_2O_4$ was used as a positive electrode. As a result, the potential window can be extended up to 1.8 V after optimizing the positive/negative electrode mass ratio and pH value of the solution. The energy density of 35 Wh/Kg was obtain based on total weight of the active electrode materials (Y. Wang & Xia, 2006).

Lithium Nitrate ($LiNO_3$) salt, Due to the use of WiSE electrolyte, it is success to develop lithium-ion battery with large electrochemical window. However, the use of WiSE electrolyte produces new concerns of the cost, high viscosity, poor wettability through electrodes and environmental hazard. Jaumaux et al. (2021) provide another inexpensive and eco-friendly inorganic lithium salt by using lithium nitrate ($LiNO_3$) salt. In addition, the WiSE electrolytes was mixed with an inert solvent (called as

diluent) in order to reduce WiSE concentration. Since the inert diluent does not change the salt solvation structure of WiSE and provide much wider ESW than WiSE electrolyte, the result of mixing WiSE electrolyte with diluent expected to preserve the electrochemical stability of WiSE electrolytes while reducing the salt concentration, decreasing the viscosity and improving the wettability. As a result, the use of $LiNO_3$ salt and 1,5-pentanediol (PD) as inert diluent can provide ESW up to 3 V by using as-developed $Mo_6S_8$ and $LiMn_2O_4$ as negative electrode and positive electrode, respectively. This is attributed to the outstanding cycling performance with an average Coulombic efficiency of 98.53% after 250 cycle (Jaumaux et al., 2021). WiSE electrolytes have been shown as one of the most extraordinary frontiers in the development of liquid electrolytes. However, the research still required more research to fulfil the limitation of the WiSE electrolytes (e.g., low conductivity and the high viscosity). Thus, the challenging and the promising future research directions towards developing realistic high power and energy density of LIBs and SCs still remained open.

Lithium Chloride (LiCl) salt, Although, LiTSFI salt progress significantly showed a high potential voltage, the practical applications for making energy storage was doubtful due to its extremely high production cost. Therefore, Turgeman et al. (2021) demonstrated that the cost-effective water-in-salt electrolyte by using lithium chloride salt (LiCl) instead of LiTSFI. In this research, LiCl salt was dissolved in water giving a saturated concentrations up to 14 M (~20 m). The use of LiCl electrolyte provided the ESWs around 2.15 V with $TiO_2$ as an anode material and $LiMn_2O_4$ (LMO) as a cathode (Turgeman et al., 2021). Though LiCl salt was open an alternative way toward formulation of new and cost-effective WiSE electrolyte, the presence of $Cl^-$ can corrode Al current collector due to the effect of the standard reduction potential (H. B. Han et al., 2011). Since Al foil widely used as a cathode current collector in the commercial Lithium-ion batteries, it is a prerequisite that any salt of lithium for Li-ion batteries must be noncorrosive towards Al.

Lithium bromide (LiBr) salt (Lu, Tu, Shu, & Archer, 2015) examine the efficacy of lithium bromide (LiBr) salt additions in propylene carbonate (PC), a commonly used liquid electrolyte, in enhancing the stability of lithium electrodeposition. Through galvanostatic cycling tests, we have determined that the

inclusion of LiBr in PC results in a more than 20-fold increase in the lifespan of the cell compared to the control LiTFSI/PC electrolyte. Batteries that have an electrolyte with 30 mol% LiBr additives are capable of cycling consistently for a minimum of 1.8 months without any instances of cell failure. The galvanostatic polarization studies indicate that an electrolyte with a LiBr concentration of 30 mol% exhibits the highest enhancement in lifespan. The presence of bromine-containing Solid Electrolyte Interface (SEI) layers greatly inhibits the production of uneven lithium electrodeposits.

Lithium iodide (LiI) salt, as described by Wu et al. in 2014, shows potential as an electrolyte addition for lithium-sulfur batteries. It stimulates the creation of protective coatings that allow the passage of Li-ion on both the positive and negative electrodes. These coatings inhibit the dissolution of polysulfides on the cathode and the reduction of polysulfides on the anode. LiI addition not only improves the stability of the cell cycle, but also reduces the cell overpotentials(F. Wu et al., 2014).

### 2.5 Water-in-Salt applied in Pouch Cell

Various designations of materials used in the construction of electrochemical capacitors make them suitable in wide range of application with high demand. Coin cells are used in most laboratory-scale of energy storage experiments because they are easy to handle, lightweight, inexpensive, and suitable for small devices (Dörfler et al., 2020; Stoller et al., 2011). However, it is limited by the specific energy output. In industry, production scaling is still ongoing. Pouch cells seem to be more suitable for maximizing specific energy because of its cell packaging light weight. In addition, specific energy can be increased by stacking of electrodes. The higher the stack, the more electrode area and thus the higher of the specific energy (Dörfler et al., 2020; Yang et al., 2020).

The design of cell and internal structure level are composed of cell internal structure, shape, and size. Typically, the LICs cell consists of 100-1000 packs of individual cell which are connected in series or parallel in order to reach energy or power requirement (Das, Li, Williams, & Greenwood, 2018). The design generally depends on the production equipment, process development, vehicle requirement and so on. In addition, the design could be constructed by determining the internal current

distribution and temperature control for battery protection (Yeow, Teng, Thelliez, & Tan, 2012).

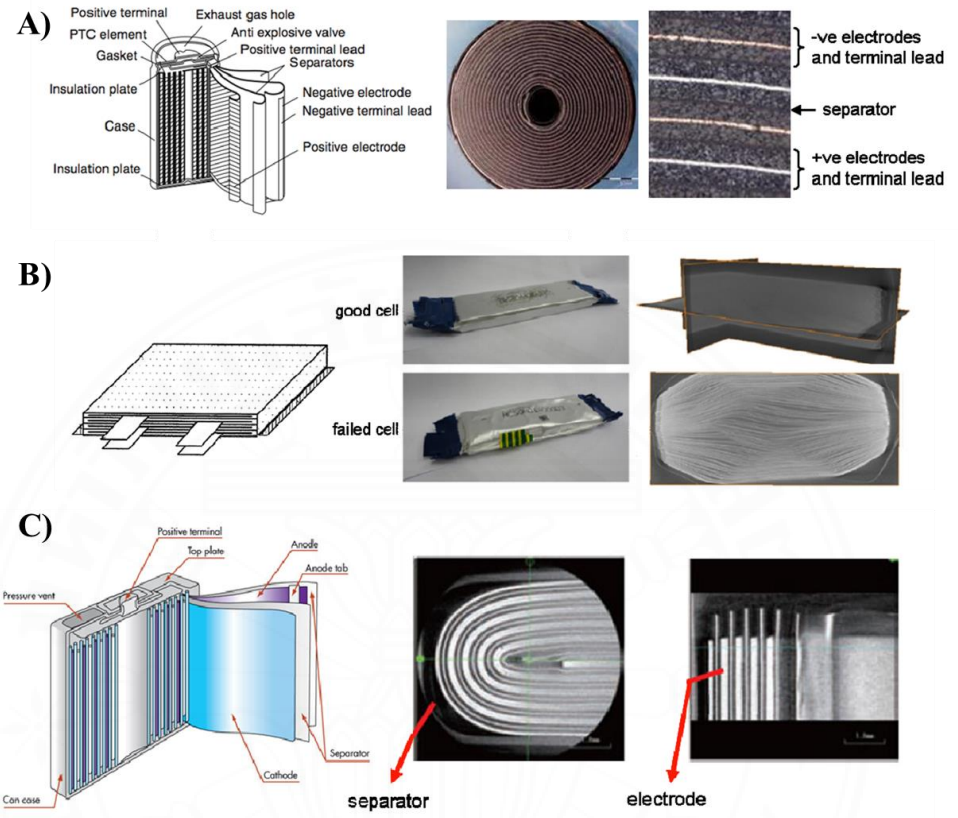


**Figure 2.5** a) Spiral wound structure for a cylindical cell and cross-sectional optical image of spiral wound core, b) Multi-stact layer of pouch cell and cross-sectional image of internal stack layer, and c) prismatic cell and cross-sectional X-ray image (Yeow et al., 2012).

Depending on the structure and form factors, lithium-ion cells can be manufactured as A) cylindrical cells, B) pouch cell, and C) prismatic cell. Choice of connecting methods is largely based on the type of cell used, and subsequently, to achieve electrical, thermal, and mechanical key criteria.

Regardless of the electrode materials, the electrolytes are often the target to determine the electrochemical performance of the electrochemical system (Forghani & Roberts, 2021). As mentioned earlier, WiSE electrolytes have attracted the attention of researchers in developing the electrochemical performance of energy storage systems.

In WiSE electrolyte system, the weight or volume ratio of salt is larger than that of water. Therefore, the chemical activity of water molecules is less restricted. WiSE then showed the remarkably enhanced the ESWs. Although many research papers reported the preparation and characterization of WiSE, the application perspective of WiSE is barely determined. According to Xu et al (2022), the characteristics of electrochemical properties were investigated by using WiSE in a pouch cell capacitor (Xu et al., 2022). The pouch cell composition was prepared by using CO $(NH_2)_2$, LiTFSI, additive KOH and water, respectively. The electrode material chosen was $Li_4Ti_5O_{12}$ as the negative electrode and $Li_{1.5}Mn_2O_4$ as the positive electrode. The ternary electrolyte system (LiTFSI- KOH-CO $(NH_2)_2$-H2O) enables the $Li_{1.5}Mn_2O_4$‖$Li_4Ti_5O_{12}$ pouch cells to extend their potential window up to 3.3 V. In addition, the capacity retention can be as high as 92 percent after 470 cycles (Xu et al., 2022).

# CHAPTER 3
# METHODOLOGY

## 3.1 Equipment and Chemicals

### Equipment

- Glassy carbon (IS-3MM.GC.WE.1) with a surface area of 0.071 $cm^2$
- Potentiostat (Palmsens4, Netherlands) with a three-electrode system.
- Conductivity&pH meter (Mettler Toledo, Greifensee, Switzerland)
- Ubbelohde Viscometer (ISO/TR 3666, 0.17%)

### Chemicals

- Lithium chloride (LiCl, 98% purity) were purchased from Kemaus.
- Lithium bromide (LiBr, 99% purity) were purchased from Acros.
- Lithium iodide (LiI, 99% purity) were purchased from Sigma-Aldrich.
- Lithium nitrate ($LiNO_3$, 99.9% purity) were purchased from Acros
- Lithium sulfate ($Li_2SO_4$, 99.9% purity) were purchased from Acros
- Lithium bis(trifiuoromethane-sulfonyl) imide (LiTFSI, 99.9% purity) were purchased from Sigma-Aldrich.
- Commercial activated carbon (YEC-8A, ~10 μm particle size, surface area ≥2000 $m^2g^{-1}$) was purchased from Fuzhou Yihuan Carbon, P.R. China.
- Carbon black super-p (99.9% Purity) was purchased from Alfar Aesar.
- Polyvinylidene fluoride (PVDF, powder 99.9% purity) was purchased from Alfar Aesar.
- N-methyl-2-pyrrolidone (NMP, ≥99% purity) was purchased from LOBA.

## 3.2 Preparation of "Water-in-salt" Electrolyte

Electrolytes were prepared by molality (mol $kg^{-1}$), which was abbreviated as m. The aqueous electrolytes were prepared using deionised water (Resistivity at 25°C is 18.2 MΩ.cm). The concentration of each electrolyte is reported as follow: LiBr (1 m, 5

m, 10 m and 15 m), LiI (1 m, 5 m and 10 m), LiCl, $LiNO_3$ and LiTFSI (1 m, 5 m, 10 m, 15 m and 20 m), $Li_2SO_4$ (1 m, 2 m and 3 m) electrolytes, respectively.

**Table 3.1** The solubility of LiCl, LiBr, LiI, $LiNO_3$, $Li_2SO_4$, and LiTFSI electrolytes.

| Electrolytes | Solubility |
|---|---|
| **LiCl** | 102.17 g/100 mL (25 °C) //24.10 m |
| **LiBr** | 180.64 g/100 mL (25 °C) //20.80 m |
| **LiI** | 164.63 g/100 mL (25 °C) //12.30 m |
| **$LiNO_3$** | 172.36 g/100 mL (25 °C) //25.00 m |
| **$Li_2SO_4$** | 34.08 g/100 mL (25 °C) //3.10 m |
| **LiTFSI** | 602.89 g/100 mL (20 °C) //21.00 m |

Based on Table 3.1, the solubility property is the determining factor for selecting the concentration for experimentation. Additionally, the crystallization properties of each salt hindered the execution of experiments at the highest concentration.

### 3.3 Measurement of electrolyte properties

The kinematic viscosity pH and ionic conductivity of LiCl, LiBr, LiI, $LiNO_3$, $Li_2SO_4$, and LiTFSI electrolytes were measured using a Ubbelohde Viscometer (ISO/TR 3666, 0.17%), pH and a conductivity meter (Mettler Toledo, Greifensee, Switzerland) respectively, with measurements taken as a function of electrolyte concentration. The solubility of these electrolytes is dependent on the temperature and the type of solvent. Table 3.1 presents the solubility limits of these electrolytes in water at specific temperatures, while Table 3.2 provides an overview of the properties of electrolytes.

**Table 3.2** Show the properties of a lithium electrolyte based on the expected concentration (m).

| Electrolytes | Concentration (m) | Density (g/mL) | Ionic conductivity (mS/cm) | pH | Viscosity (cP) |
|---|---|---|---|---|---|
| **LiCl** | 1 | 1.03 | 72.25 ± 0.05 | 0.87 ± 0.02 | 1.08 ± 0.02 |
| | 5 | 1.10 | 178.87 ± 0.29 | 1.45 ± 0.01 | 1.79 ± 0.02 |
| | 10 | 1.15 | 158.67 ± 0.54 | 3.02 ± 0.01 | 3.51 ± 0.02 |
| | 15 | 1.23 | 104.40 ± 0.16 | 5.99 ± 0.02 | 7.39 ± 0.03 |
| | 20 | 1.32 | 73.94 ± 0.55 | 11.49 ± 0.39 | 13.67 ± 0.56 |
| **LIBr** | 1 | 1.06 | 55.01 ± 0.16 | 0.80 ± 0.01 | 1.00 ± 0.01 |
| | 5 | 1.23 | 183.57 ± 0.09 | 0.91 ± 0.03 | 1.39 ± 0.04 |
| | 10 | 1.42 | 214.81 ± 0.14 | 1.38 ± 0.04 | 2.39 ± 0.06 |
| | 15 | 1.59 | 150.55 ± 0.23 | 2.60 ± 0.08 | 4.51 ± 0.15 |
| **LiI** | 1 | 1.08 | 62.63 ± 0.09 | 9.49 ± 0.02 | 0.98 ± 0.01 |
| | 5 | 1.42 | 192.97 ± 0.26 | 8.39 ± 0.13 | 1.31 ± 0.01 |
| | 10 | 1.72 | 172.93 ± 1.13 | 7.37 ± 0.01 | 1.95 ± 0.01 |
| **$LiNO_3$** | 1 | 1.05 | 52.50 ± 0.04 | 0.73 ± 0.01 | 0.85 ± 0.01 |
| | 5 | 1.16 | 125.04 ± 0.05 | 0.78 ± 0.01 | 1.06 ± 0.02 |
| | 10 | 1.26 | 156.37 ± 0.30 | 1.72 ± 0.03 | 2.28 ± 0.04 |
| | 15 | 1.34 | 166.55 ± 0.28 | 3.05 ± 0.02 | 4.16 ± 0.02 |
| | 20 | 1.40 | 153.01 ± 0.21 | 3.29 ± 0.05 | 4.89 ± 0.07 |
| **$Li_2SO_4$** | 1 | 1.03 | 32.21 ± 0.28 | 0.83 ± 0.02 | 1.02 ± 0.02 |
| | 2 | 1.09 | 81.61 ± 0.05 | 1.25 ± 0.01 | 1.40 ± 0.02 |
| | 3 | 1.18 | 83.58 ± 0.13 | 2.10 ± 0.03 | 2.72 ± 0.04 |
| **LiTFSI** | 1 | 1.09 | 20.01 ± 0.22 | 1.26 ± 0.01 | 1.36 ± 0.01 |
| | 5 | 1.42 | 50.03 ± 0.12 | 2.91 ± 0.12 | 3.67 ± 0.16 |
| | 10 | 1.54 | 31.78 ± 0.38 | 5.79 ± 0.14 | 8.44 ± 0.21 |
| | 15 | 1.69 | 19.17 ± 0.27 | 13.38 ± 0.26 | 22.65 ± 0.41 |
| | 20 | 1.71 | 10.43 ± 0.06 | 26.52 ± 0.03 | 34.18 ± 0.06 |

For an accurate calculation, the viscosity (ν mm²/sec) is calculated based on the equation (3.1) where constant K is 0.00993 mm²/sec, t is the running time.

$$\nu = K \times t \tag{3.1}$$

$$\nu = \frac{\eta}{\rho} \tag{3.2}$$

where, $\nu$ is Kinematic viscosity, $\eta$ is Dynamic viscosity and $\rho$ is Density

The concept of surface tension ($\gamma$) has a significant role in electrochemical applications. Because many electrochemical systems involve physical and chemical changes occurring at the boundaries between solid materials and liquids. In discussion, the idea of surface tension and its relevance in the context of specific measurement techniques, like determining the contact angle of water. Essentially, surface tension in liquids leads to the creation of droplets, due to various attractive forces between the molecules. The pendent drop method is commonly used to measure surface tensions of liquids. These forces include interactions like dipole-to-dipole, dipole-to-induced dipole, hydrogen bonding, and dispersion. Because of differences in surface energies at the interface between different materials(Bengt Kronberg, Krister Holmberg, & Bjorn Lindman, 2014). The surface tension at each of the interfaces can be calculated by taking the value of $\gamma_{lv}$ from the pendant drop method and applying Young's equation (3.3) (Hunter, White, & Chan, 1987).

$$W_{sl} = \gamma_{lv}(1 + \cos\theta) \tag{3.3}$$

Where $\gamma_{lv}$ is liquid-vapor interfacial tensions which can be obtained from the obtained pendent analysis using the ImageJ software based on the Young-Laplace equation.(Daerr & Mogne, 2016; Eugene Huang, 2021)

### 3.4 Preparation of activated carbon electrode

Commercial activated carbon (YEC-8A, ~10 μm particle size, surface area 1,955 $m^2 g^{-1}$) was purchased from Fuzhou Yihuan Carbon, P.R. China. Carbon black super P (99.9% Purity) and Polyvinylidene fluoride (PVDF, powder 99.9% purity) were purchased from Alfar Aesar. N-methyl-2-pyrrolidone (NMP, ≥99% purity) was purchased from LOBA. Activated carbon (AC) electrodes were used as a model electrode for evaluate the electrochemical properties of the electrolyte. The working electrodes were prepared by mixing 85 wt% AC powder, 5 wt% carbon black, 10 wt% PVDF, and NMP (80% by weight)(Inal & Aktas, 2020). The mixture was stirred using a vortex mixer for 30 minutes to obtain a homogeneously mixed carbon slurry. The obtained slurry was in a thick liquid form. The slurry was then applied to the surface of a glassy carbon electrode (diameter of 3 mm) to cover its surface area, and the solvent was evaporated at 60°C for 3 hours (Shabeeba, Thayyil, Pillai, Soufeena, & Niveditha, 2018). For the preparation of activated carbon electrode, coin cell assembly, the carbon slurry was spread onto a prepared anti-corrosion Al current collector with a doctor blade device to produce a carbon film with a wet thickness of 250 μm. The cast carbon electrode was then dried in an oven at 60 ºC for 5 h, and left under room temperature overnight. The dried electrode was then compressed by the roller machine to achieve a dense electrode. the prepared electrodes were cut to the predetermined size for coin cell 2016. Then, the as-prepared separator was placed between the two electrodes. Two electrodes were aligned to maximize the overlapping area of carbon coating. The electrolyte from “dilute” to “superconcentrated” was filled to the supercapacitor cell. Note that the hydrolyzed polyethylene (HyPE, purchased from Gelon LIB. Group, china) were used as a representative of the commercial separator for comparing the supercapacitor performance(Deerattrakul et al., 2023).

### 3.5 Electrochemical measurements

All the electrochemical measurements cyclic voltammetry (CV), and electrochemical impedance spectroscopy (EIS) analyses were performed by using a potentiostat (Palmsens4, Netherlands) with a three-electrode system. In the three-electrode system, the electrochemical properties of electrolytes were investigated using activated carbon. Glassy carbon with the as- coated AC were used as standard working

electrodes. Platinum wire and Ag/AgCl were used as counter and reference electrodes, respectively. Each CV performed at scan rate 10 to 100 $mV.s^{-1}$ performed at room temperature ($25^{o}C$). To determine the potential window for a cyclic voltammetry (CV) curves (see Figure 3.1), the following steps were taken: a horizontal line was drawn at the point where the y-axis intersects zero, and the two points where the CV curve intersects the horizontal line were identified, one on the negative side and one on the positive side (Akgul, Üzdürmez, Kamış, Kılıç, & Demir, 2021). The potential window was then determined by measuring the distance between the onset of the peak and the point where the CV curve intersects the horizontal line on both the positive and negative sides. The peak width was obtained by measuring the distance between these two points.

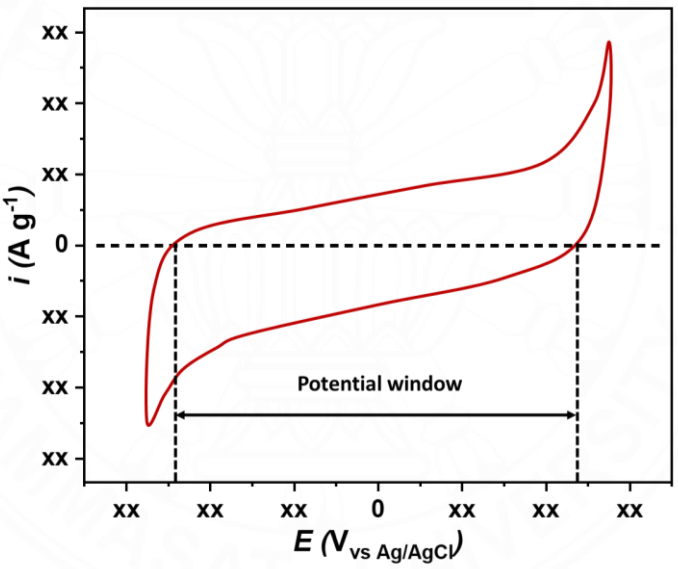


**Figure 3.1** The CV curve showing the determination of the potential window in aqueous electrolytes.

The gravimetric capacitance calculated from CV curves was based on the equation (3.4)

$$C_{CV} = \int \frac{IdV/v}{2m\Delta V} \tag{3.4}$$

where $\int IdV$ is the area of the CV closed curve, $v$ is the electrode potential scan rate (V $s^{-1}$), $m$ is the mass loading of the active material on the electrode (g), $\Delta V$ is the potential window (V).

From the GCD cycling, the gravimetric capacitance of the supercapacitor can be calculated using equation (3.5)

$$C_{GCD} = 4 * \frac{I\Delta t}{m\Delta V} \tag{3.5}$$

where $C_{GCD}$ is the gravimetric capacitance of the symmetric supercapacitor (F $g^{-1}$), $I$ is the applied current (A), $\Delta t$ corresponds to the discharging time (s), $\Delta V$ is the potential range (V) and $m$ the total mass of active material of both electrodes (g).
The specific energy density ($E$) and specific power density ($P$) at various current densities were calculated using the following equations

$$E = \frac{1}{8} \times \frac{1000}{3600} \times C_{cv} \times (\Delta V)^2 \tag{3.6}$$

$$P = \frac{E \times 3600}{\Delta t} \tag{3.7}$$

where $\Delta t$ is the discharge time (s), and $m$ is the mass loading of the active material on one electrode. Note, all the gravimetric capacitance values discussed in this work refer to the discharge process.

Electrochemical impedance spectroscopy (EIS) was performed at 0.0 V using an amplitude of 10 mV perturbation in the frequency range of 10 mHz to 100 kHz (Hirunpinyopas, Iamprasertkun, Le Fevre, et al., 2022). To understand the behavior of the electrolytes across a range of frequencies, it is necessary to calculate the capacitance as a function of frequency, taking into account both the real ($C'_{(\omega)}$) and complex ($C''_{(\omega)}$) components using equations (3.8) and (3.9)(Taberna, Simon, & Fauvarque, 2003). The low frequency values of $C'$ orresponds to the capacitance of the system during discharge, while $C''$ corresponds to the irreversible energy losses.

$$C'_{(\omega)} = \frac{-Z''_{(\omega)}}{\omega \left| Z_{(\omega)} \right|_2} \tag{3.8}$$

$$C''_{(\omega)} = \frac{Z'_{(\omega)}}{\omega \left| Z_{(\omega)} \right|_2} \tag{3.9}$$

The normalised real and complex capacitances as a function of frequency are plotted for each of the analysed electrolytes.

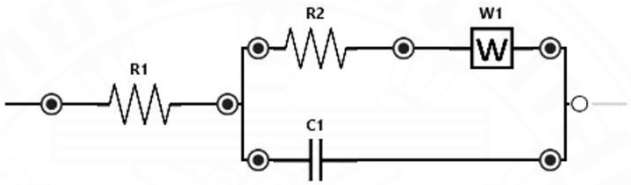


**Figure 3.2** Equivalent circuits used for fitting of impedance data.

# CHAPTER 4
# RESULT AND DISCUSSION

This chapter is divided into two main parts on discussion: (4.1) Revisiting the Properties of Lithium Chloride as a “Water-in-salt” Electrolyte for Pouch Cell Electrochemical Capacitors characterization (4.2) A Comprehensive Study of Affordable 'Water-in-Salt' Electrolytes and Their Properties

## 4.1 Revisiting the Properties of Lithium Chloride as “Water-in-salt” Electrolyte for Pouch Cell Electrochemical Capacitors

In recent years, there has been a significant focus on finding alternative electrolytes, particularly the "water-in-salt" electrolyte known as lithium bis (trifluoromethanesulfonyl) imide (LiTFSI), which has gained attention in the field of high-voltage electrolytes. However, the "water-in-LiTFSI" system is characterized by much higher expenses and lower efficiency in terms of ionic transport, in comparison to aqueous solutions containing lithium halide, nitrate, and sulphate salts. This study revealed the characteristics of a "water-in-salt" substance created using a highly concentrated 20 m (equal to 14.28 M) lithium chloride electrolyte. The electrolyte underwent testing with several carbon-based materials as a model system, and the results were subsequently used to a pouch cell supercapacitor. Research has shown that the utilization of highly concentrated LiCl can increase the potential range of the supercapacitor in both half-cell electrodes (about 3.0 V) and pouch-cell devices (1.4 V measured at 100 mV $s^{-1}$). This study provides a comprehensive understanding of the physical and electrochemical characteristics of LiCl, which could potentially be used as an affordable "water-in-salt" electrolyte in energy storage, as an alternative to LiTFSI.

### 4.1.1 Electrolyte Properties

The electrolyte in this experiment was prepared using high-purity LiCl in the aqueous system using Milli-Q water (18.2 MΩ·cm at 25 ºC), the concentration was varied from 1 m to 20 m (in molality unit). It is obvious that the mole fraction between

water and $Li^+$ significantly decreases from 55.5 to 2.7 when dissolving more amount of LiCl. This number indicates the highest possible water molecules that surround neat $Li^+$ (hydrated shells). Our observation on the ratio of a free water molecule: cation was also close to the previous literature (Iamprasertkun, Ejigu, & Dryfe, 2020; Suo et al., 2015; Wang, Meng, Sun, Liu, & Hou, 2020), confirming the existence of "water-in-salt" behaviour in LiCl electrolyte. It is noted that the alter of solvation state of the prepared electrolyte and the schematic illustration of the electrolyte structure being transition from "salt-in-water" to "water-in-salt" is given in Figure 4.1 where the extended solvation structure were previously reported in the following literature.

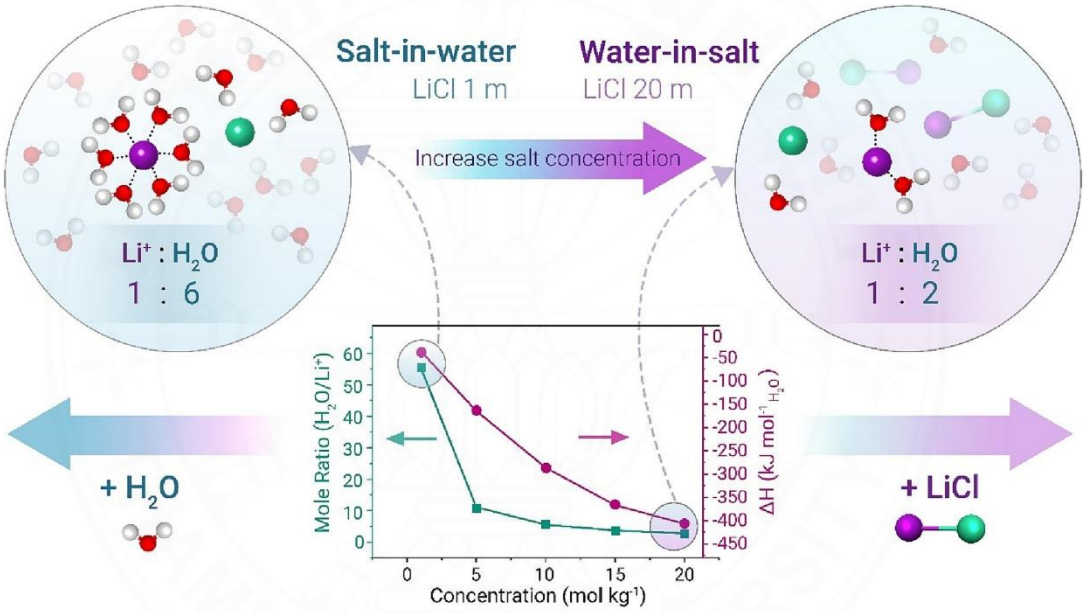


**Figure 4.1** Schematic illustration of the diminished electrolyte solvation from "salt-in-water" to "water-in-salt" where the typical Li+ surround by six molecules of water. The maximum $H_2O$: $Li^+$ became significantly decreasing once adding more salt, achieving 2.7 for "water-in-salt" conditions. The enthalpy of mixing with respect to the concentration is presented in the purple line.

However, adding more LiCl caused the amplifying in the density of the as-prepared electrolyte as can be seen in Table 4.1 (density increase up to ~30% for the highest concentration). Since Arrhenius explored the properties of electrolyte solution in the 1880s, it is reported that the viscosity of the electrolyte depends on the salt type and the concentration. At the low concentration (below 0.1 M), the increase of

electrolyte concentrations leads to the reduction of viscosity according to the Einstein principles of hydrodynamics and the finding from Falkenhagen and Dole(D. E. Goldsack & R. Franchetto, 1977). On the other hand, Goldsack and Franchetto demonstrated that the viscosity of the electrolyte increases with respect to the salt concentration when the salt concentration is above 0.1 M(D. E. Goldsack & A. A. Franchetto, 1977; D. E. Goldsack & R. Franchetto, 1977). This is in excellent agreement with our result shown in Table 5. It is no doubt that the viscosity enlargement of LiCl could lower the ionic transport of lithium ion (Iamprasertkun et al., 2020; Kim, Wu, Morrow, Yethiraj, & Yethiraj, 2012); however, our presented LiCl "water-in-salt" exhibits three times lower viscosity than that of conventional LiTFSI. Note that the information on viscosity with respect to the electrolyte concentration of 1:1 "salt-in-water" was clearly presented by Goldsack, especially the concentration below 6 m

**Table 4.1** The properties of the electrolyte from "salt-in-water" to "water-in-salt".

| Electrolyte | m (mol $kg^{-1}$) | Density (g $mL^{-1}$) | $H_2O$: $Li^+$ ratio | Conductivity (mS $cm^{-1}$) | Viscosity (cP) | Potential window (V) |
|---|---|---|---|---|---|---|
| LiCl | 1 | 1.03 | 55.5 | 72.25 ± 0.05 | 0.97 ± 0.02 | 1.50 |
| | 5 | 1.10 | 11.1 | 178.87 ± 0.29 | 1.73 ± 0.01 | 1.85 |
| | 10 | 1.15 | 5.55 | 158.67 ± 0.54 | 3.77 ± 0.02 | 2.30 |
| | 15 | 1.23 | 3.70 | 104.40 ± 0.16 | 7.98 ± 0.03 | 2.50 |
| | 20 | 1.32 | 2.78 | 73.94 ± 0.55 | 16.43 ± 0.56 | 2.60 |
| LiTSFI | 1 | 1.05 | 55.5 | 19.96 ± 0.22 | 1.43 ± 0.01 | 1.85 |
| | 5 | 1.18 | 11.1 | 50.03 ± 0.12 | 3.72 ± 0.16 | 2.00 |
| | 10 | 1.35 | 5.55 | 31.92 ± 0.38 | 8.46 ± 0.21 | 2.15 |
| | 15 | 1.50 | 3.70 | 19.09 ± 0.27 | 21.74 ± 0.41 | 2.30 |
| | 20 | 1.72 | 2.78 | 10.41 ± 0.06 | 49.41 ± 0.06 | 2.50 |
| **LiTFSI*** | 21 | – | – | 8.2 | – | 3.00 |
| **$LiTFSI/(H_2O)_{2.6}(CH_3CN)_3$**** | 5 | – | – | 17.4 | – | 3.00 |
| **LiTFSI hydrogel***** | 10 | – | – | 51.3 | – | 2.60 |

Note, *Reference (Suo et al., 2015), **Reference (Dou, Lei, Wang, Zhang, Xiao, Guo, Wang, Yang, Li, & Shi, 2018), and ***Reference (Dai, et al., 2019).

To further explain the properties of the as-prepared “water-in-salt”, the ionic conductivity of LiCl and LiTFSI. Interestingly, it is found that LiCl electrolyte displays higher ionic conductivity than that of the LiTFSI electrolyte in all concentrations. The highest ionic conductivity is obtained in the same concentration (5 molalities) for both LiCl and LiTFSI electrolytes. Our observation is in the same direction as the “water-in-salt” prepared using $NaClO_4$, reported by (Sakamoto et al., 2020), and (Yin, Zheng, Qi, & Wang, 2011). For the diluted concentration (below 0.01 M), there is a limiting molar conductance; hence, the ionic conductivity of the dilute electrolyte is then followed the Debye–Hückel theory(C. da Silva et al., 2022). However, it can be expected that the electrolyte conductivity can be higher as increasing the concentration due to the rise of free ions, which is also observed in the previous literature(Xi Wu et al., 2019). The solvent (water) can be represented as a continuous medium, exhibiting the space for the free ions; then, the conductivity depends on the amount of the ions and their transport properties. This is because there are sufficient free spaces for the cations/anions; therefore, the effect of the ionic association and the ionic hydration is then negligible. Wu et al., also reported that the trend of electrical conductivity kept increasing until reaching the peak value at about 3 m (Xi Wu et al., 2019), this is somewhat similar to our observation where the electrical conductivity reached a peak value at 5 m. For the concentration above 5 m where more ions exist in the electrolyte solution, the hydration and ionic association of the electrolyte become significant. This was well described by Robinson–Harned, and Krumgalz for localized hydro/solvolysis (B. Krumgalz, 1974; B. S. Krumgalz, 1982), and Bjerrum’s ion theory (Fuoss, 1978; Xi Wu et al., 2019). This influent is then diminished the electrical conductivity when applied to higher concentration, this is due to the ion pair interaction, in which the charge becomes close to one another (McEldrew, Goodwin, Bi, Kornyshev, & Bazant, 2021). At this stage, it could be concluded that the LiCl electrolyte displays a superior property when compared to the LiTFSI electrolyte. However, it is noted that the pH of “water-in-salt” either LiCl or LiTFSI is in acidic conditions (pH ~6.7 for LiCl and ~5.0 for LiTFSI), which could damage a traditional aluminium current collector. Thus, we then applied the anti-corrosion graphite protective layer for the preparation of large-

scale devices (Chomkhuntod, Iamprasertkun, Chiochan, Suktha, & Sawangphruk, 2021).

### 4.1.2 Extended Electrochemical Properties of Model Electrodes

Apart from the physical properties, the electrochemical properties of the prepared WISEs were then evaluated in three electrode configurations using three types of carbon model electrodes: (1) glassy carbon, (2) graphite rod, and (3) activated carbon Overall, the window potential of the electrolytes was evaluated by the area without any gas evolution reactions e.g. oxygen evolution (OER), chlorine evolution (CER), and hydrogen evolution (Nualchimplee et al., 2022). Once the salt concentration (LiCl) was increased, the potential window was then expanded. This is because the diminished $Li^+/H_2O$ molar ratio leads to an insufficient water shell among $Li^+$ species; hence, the oxygen/hydrogen evolution potential was then shifted to more positive and negative potentials, respectively (Coustan, Shul, & Bélanger, 2017). This is in good agreement with the electrochemical properties of LiTFSI WISEs, reported by (Coustan et al., 2017). For the positive limit, it is suggested that the potential window can be limited by either OER (Lannelongue et al., 2018; Park, Lee, & Kim, 2021) or CER (Karlsson & Cornell, 2016; Vos et al., 2019), the negative end of the CV might be limited by the HER (Gambou-Bosca & Bélanger, 2016; Iamprasertkun et al., 2020; Suo et al., 2015; Suo et al., 2016). Interestingly, LiCl could serve as a WISE in all model systems as shown in Figure 9, with the transition from “salt-in-water” to “water-in-salt”. The operating window potential is then enlarged. There are some faradic processes presented in the case of applying a graphite rod as a working electrode as shown in Figure 4.2b. This suggests that the reduction of lithium electrolyte may occur on the graphite electrode (refer to the reduction potential at −0.5 V vs. Ag/AgCl). It is reported that the lithium reduction into the graphite bulk starts at −0.5 V to −1.4 V (for a molten LiCl salt), in which the rate of this reaction is controlled by the diffusion of lithium into graphite galleries (Q. Xu, Schwandt, Chen, & Fray, 2002). Furthermore, the reductive peak at the positive branch (about 0.8 V vs Ag/AgCl) was suggested to be gas reduction reaction. This process was confirmed by purging $N_2$ gas into the electrolyte and the CVs at 100 mV $s^{-1}$ were carried out in the seal-saturated $N_2$ chamber. Clearly, it is evident that there is no reductive peak presented for the $N_2$ purged conditions while the

CVs of the electrolyte without $N_2$ purged show the reductive process between 0.8 and 0.9 V vs. Ag/AgCl. It is also observed that the increase of electrolyte concentrations leads to the reduction of the displayed current in the CVs as the two effects (including the capacitance and the voltage) are competing; however, the increase of voltage could result in higher energy density when compared to the capacitance. By consider the Nernst-Planck equation both electrolyte concentration and ionic diffusion are involved in the current density (Albrecht, Gibb, & Nuttall, 2013), it is also noticeable that once the concentration is higher, the currents are suppressed. This is because the diffusion of electrolytes shrinks in an order of magnitude when being transitioned from "salt-in-water" to "water-in-salt", which can be observed in the previous literature (Iamprasertkun et al., 2020). The decrease in the diffusion coefficient leads to the reduction of the displayed current.

The electrochemical potential window of that glassy carbon, graphite rod, and activated carbon is summarised in Figure 4.3. Overall, the scan rate plays a significant role in the voltage window, the voltage window decreases as increase the scan rate is observed at every concentration and all samples. For glassy carbon in Figure 10a, the potential window evaluated at 10 mV $s^{-1}$ with respect to the electrolyte concentration is between 2.9 and 3.2 V. A significant voltage improvement when applied higher salt content is then found at high scan rate of 100 mV $s^{-1}$ (improved from 2.1 to 3.1 V). Besides, the graphite rod in Figure 10b shows a relatively close potential window among all scan rates. The potential window enhances from 2.7 to 2.9 V at 10 mV $s^{-1}$ and 2.5 to 2.6 V at 100 mV $s^{-1}$, respectively. In addition, the potential improvement of activated carbon (Figure 10c) is from 2.5 to 3.3 V at 10 mV $s^{-1}$ and 1.7 to 2.7 V at 100 mV $s^{-1}$, respectively. Consider at high scan rate (100 mV $s^{-1}$) and electrolyte concentration at 5 m, it is found that the graphite electrode (Figure 10b) achieves the highest potential window ~ 2.5 V due to its high crystallographic structure while the glassy carbon exhibits the turbostratic carbon structure in which the basal planes have slipped out of the alignment (McCreery, 2008; Uskoković, 2021). However, this glassy type of carbon (~2.4 V) structure exhibits fewer defects when compared with activated carbon electrode (~1.8 V) (Uskoković, 2021). The more edge defect was reported to be a highly active area for the water splitting reaction (Hirunpinyopas, Iamprasertkun, Fevre, et al., 2022).

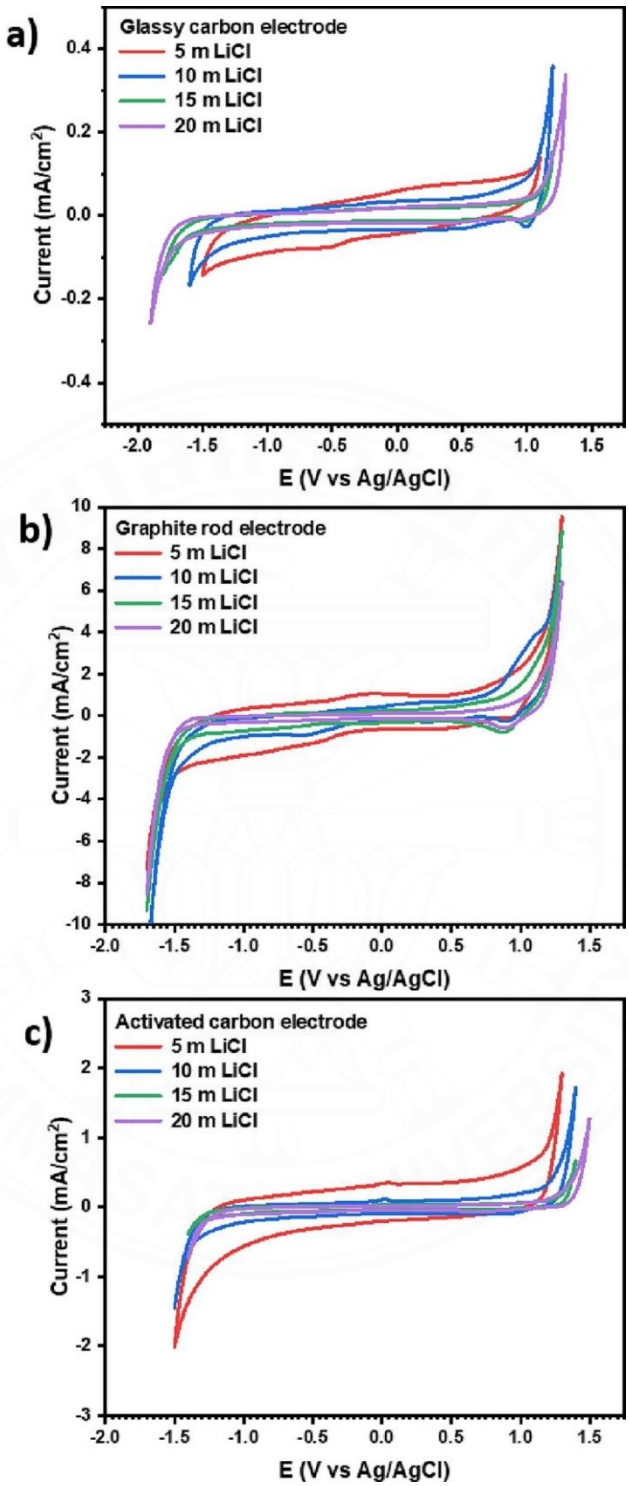


**Figure 4.2** The electrochemical response (CVs at 100 mV $s^{-1}$) of a variety of carbonaceous electrodes from "salt-in-water" to "water-in-salt" using lithium chloride as the electrolyte (a) glassy carbon, (b) graphite rod, and (c) activated carbon electrodes.

It is noted that the potential window is enlarged when apply lower scan rate due to the decreased of *iR* drop (Dou, Lei, Wang, Zhang, Xiao, Guo, Wang, Yang, Li, Shi, et al., 2018), which is agree with previous supercapacitor work (Bhoyate et al., 2017; Dou, Lei, Wang, Zhang, Xiao, Guo, Wang, Yang, Li, Shi, et al., 2018). On the other hand, the "water-in-salt" electrolyte (20 m) running at 10 mV $s^{-1}$ shows relatively close potential window among all working electrodes, approximately 3 V. This confirms that applying superconcentrated concentration can improve the voltage window no matter what electrode materials it is. At high scan rate (100 mV $s^{-1}$), the activated carbon electrode shows lowest potential window (achieving 2.5 V vs. Ag/AgCl) when compared with glassy carbon, and graphite rod. This is due to glassy carbon and graphite rod exhibiting less structural defect than that of activated carbon (McCreery, 2008; Uskoković, 2021). Applying fast charging rate, it is evident that the structural defect plays less role in the gas evolution (Hirunpinyopas, Iamprasertkun, Fevre, et al., 2022; Uskoković, 2021).

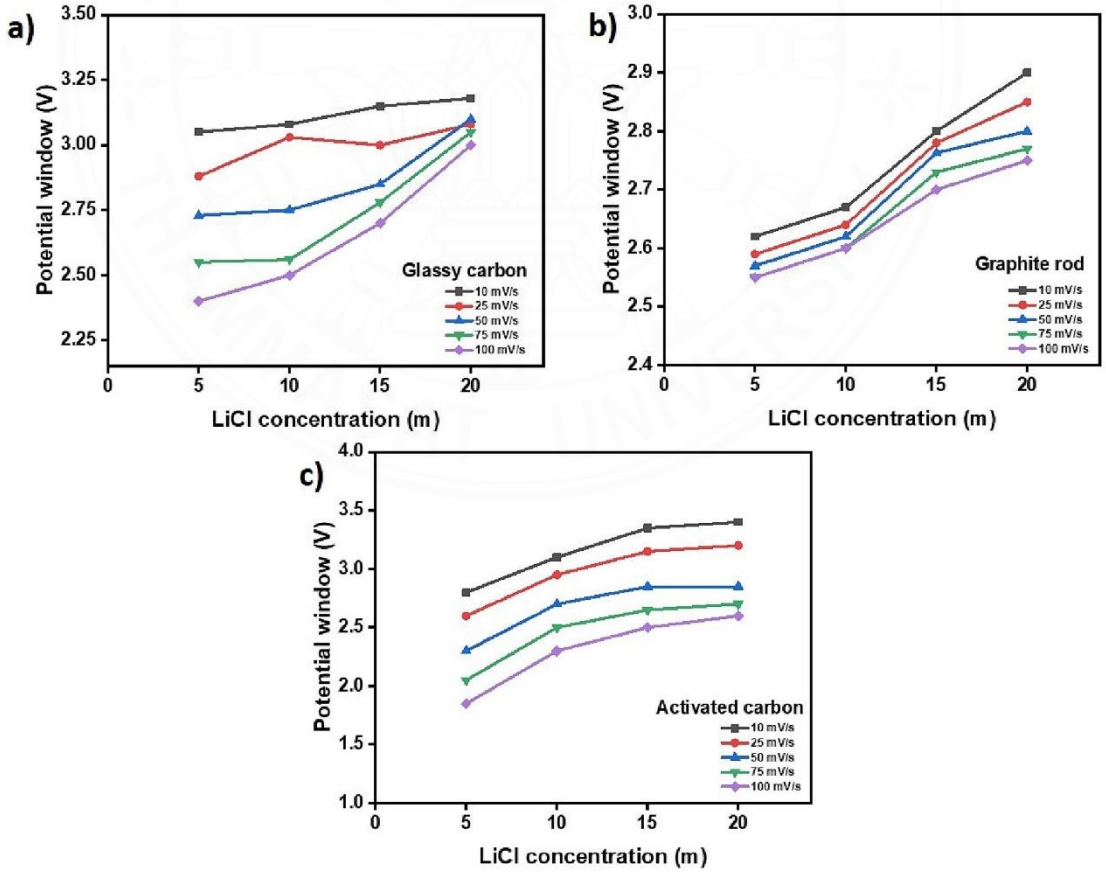

**Figure 4.3** The electrochemical potential window of the as-prepared electrolytes from "salt-in-water" to "water-in-salt" in each carbon model electrode: (a) glassy carbon, (b) graphite rod, and (c) activated carbon. Note that the concentration of "water-in-salt" electrolyte is 20 m.

### 4.1.3 Demonstrated the applicability

To confirm the applicability of LiCl as "water-in-salt" in a pouch-cell supercapacitor. We then optimised the mass/solvent ratio between the electrode materials containing activated carbon (AC), carbon black (CB), and polyvinylidene fluoride (PVDF) and solvent (*N*-Methyl-2-pyrrolidone, NMP). It is found that the slurry: NMP ratio of 20:80 exhibits the best casting condition showing a smooth surface without any air void. The as-prepared electrodes were then tested in three-electrode configurations using superconcentrated LiCl (20 m). Obviously, many reactions occurred as seen on the CV graph such as a chlorine evolution reaction, which is typically found in the alkaline-chloride based electrolyte (T. Lim et al., 2020), and the corrosion of Al substrate when applying the potential to an electrode. Hence, the traditional Al current collector with the activated carbon coated on the surface is not suitable for the "water-in-salt" environment due to the acidic properties of the electrolyte leading to aluminium corrosion. To address this issue, we then introduced a graphite protective layer coating on the traditional aluminium substrate. These graphite layers could improve the interfacial contact between electrode materials and substrate (Chomkhuntod et al., 2021). In addition, it could enhance the corrosion resistance in the aqueous medium (Chomkhuntod et al., 2021). The images of the anti-corrosion graphite sheet with the coated active materials are shown in 4.4a.

Inclusively, we successfully demonstrated the applicability of 20 m LiCl as WISEs by avoiding corrosion from the aluminium substrate. Remarks, the as-prepared electrode was then calendared before the fabrication, The voltage window (observed from CV) of the pouch-cell using 20 m LiCl in 4.4b clearly displays twice times larger than that of 1 m LiCl. The 20 m LiCl "water-in-salt" can provide a stable operating window potential of up to 1.4 V while 1 m LiCl "salt-in-water" can achieve only up to 0.8 V (in a full-cell device). This transition of CV from 1 and 20 m also agrees

with (Park et al., 2021). It should be noted that this experiment was conducted in a pouch cell level where the activated carbon, binder, and conductive additive; hence, the rolling press was then applied giving the different compactness of the electrode. We have found that the CV of the electrode (after rolling press) in 20 m LiCl also displays larger current density than that 1 m (measure using 3 electrode configuration). This suggests that the electrode compactness is involved. The electrode processing (before fabrication of the device) may affect the porosity, and density of the prepared electrode, in which may be suitable for a specific electrolyte size (here is "water-in-salt"). The "water-in-salt" electrolyte displays lower hydrated size than that of "salt-in-water". In this case, the "water-in-salt" electrolyte may access the dense and small channel of the as-fabricated electrode. For comparison, the capacitance of pouch-cell containing 20 m LiCl WISE exhibits cell capacitance of about 2.4 F $g^{-1}$ (normalised by the total mass of the cell including electrode materials, a separator, an electrolyte, and a current collector). The "water-in-salt" shows about 40 percent higher capacitance when compared to the diluted condition (1 m LiCl, $C$ = 1.7 F $g^{-1}$). It is noted that the specific capacitance of the activated carbon in the "water-in-salt" is about 100F $g^{-1}$. Obviously, this work demonstrates the strategy of using 20 m LiCl as WISEs, the performance is effectively comparable to the traditional "LiTFSI" electrolyte, which shows an operating voltage of 2.0 V (Le Fevre, Ejigu, Todd, Forsyth, & Dryfe, 2021). In addition to a CV, the impedance of those prepared pouch-cells was then evaluated at an open circuit potential as presented in 4.4 c. The pouch-cell with 20 m LiCl exhibits lower internal resistance than that of 1 m LiCl (the internal resistance of 1 and 20 m are 19 Ω and 14 Ω, respectively), and the semi-circle due to the charge transfer resistance is not presented in 20 m LiCl (see inset). Moreover, the plot of the highly concentrated electrolyte shows a straight line closer to Y-axis than that of the diluted one indicating a better capacitor behaviour (Iamprasertkun, Hirunpinyopas, Deerattrakul, Sawangphruk, & Nualchimplee, 2021; Laschuk, Easton, & Zenkina, 2021).

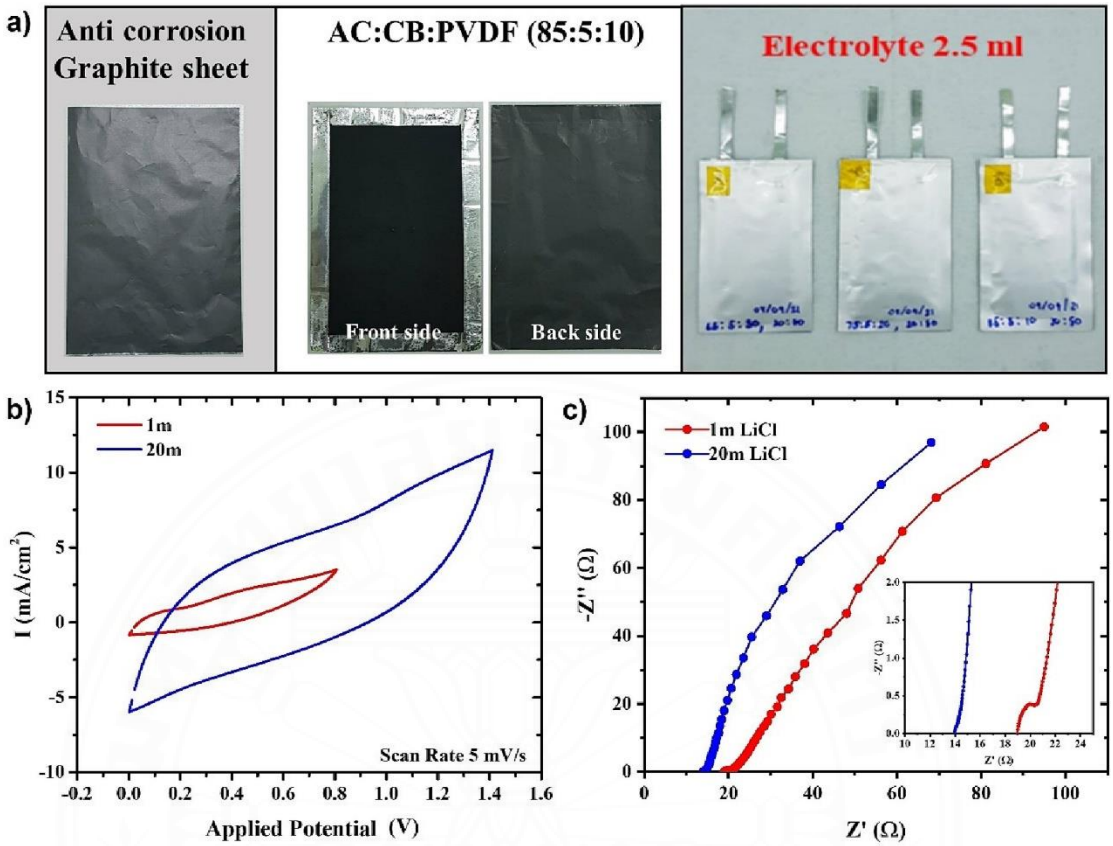


**Figure 4.4** The demonstration of using 20 m LiCl as a "water-in-salt" electrolyte in the pouch-cell device (a) images of active materials coated on the prepared anti-corrosion graphite sheet, and the prepared pouch-cell, (b) CV at 5 mV $s^{-1}$, and (c) Nyquist plot of the pouch-cell devices.

## 4.2 A Comprehensive Study of Affordable 'Water-in-Salt' Electrolytes and Their Properties

### 4.2.1 Physical Properties

The physical properties, such as viscosity**,** and conductivity of lithium electrolytes are affected by various factors, such as temperature, pressure, density**,** and concentration of the electrolyte. Once the temperature is increased in any fluid, its density decreases; hence, decreasing viscosity(Logan et al., 2018; Widegren & Magee, 2007). In this experiment, the temperature and pressure were kept at room condition (25$^{o}$C, atmospheric). The electrolyte concentration is then varied from 1 m defined as "salt-in-water" to either 20 m or at the maximum solubility of the applied salts "water-in-salt". Presents the physical properties of electrolytes for a variety of lithium-based

salts. Obviously, changing the salt content would affect the density of the electrolyte as illustrated in Figure 4.5a Once the density of the salts increases, the decrease in the mole ratio of water per Li-ion (neat) is significantly found. This is due to the reduction in the volume of water, which is surrounded by neat ions. The viscosity in Figure 4.5b was obtained from the kinematic viscosity and density.

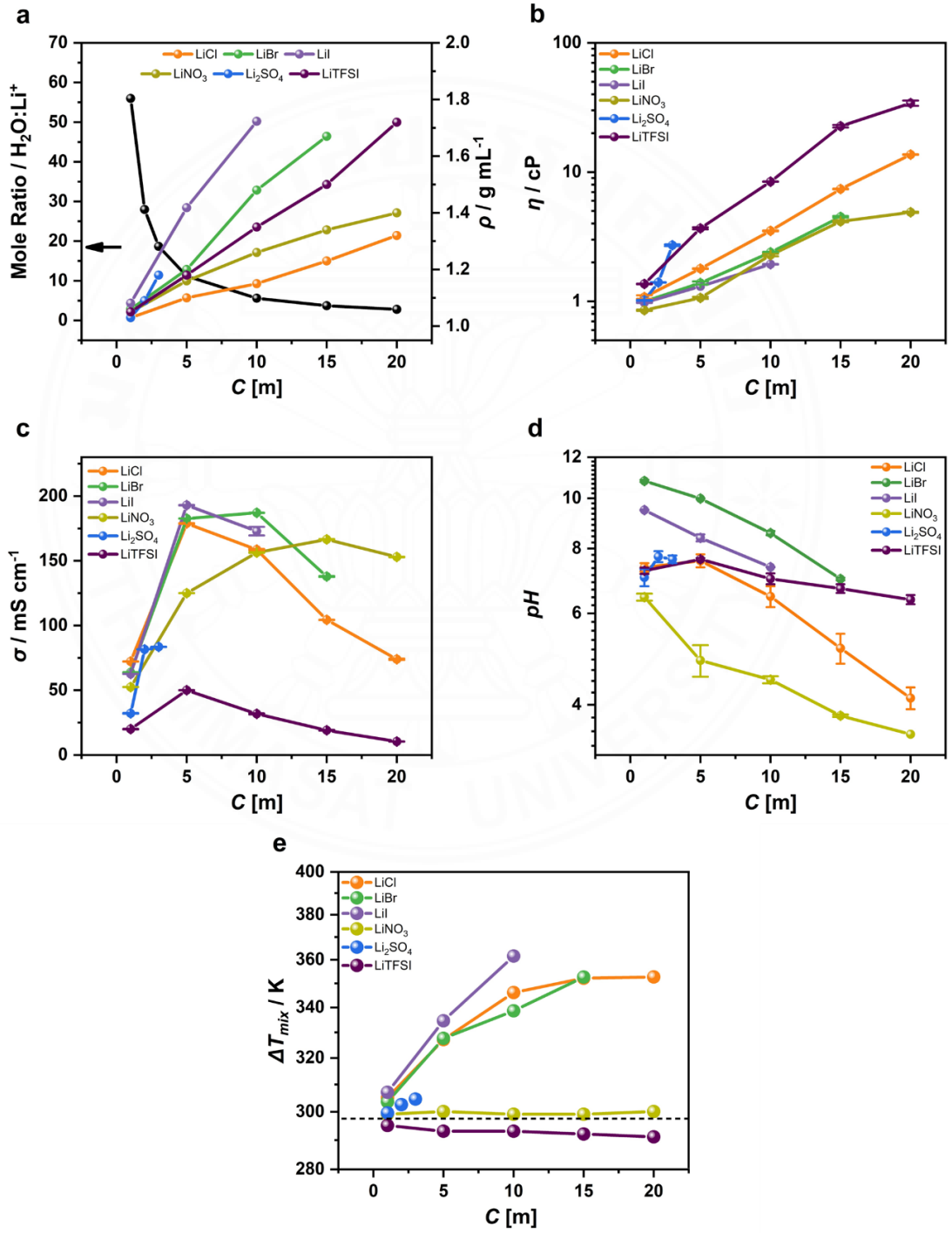

**Figure 4.5** The physical properties of the electrolyte at various concentrations (a) density comparison and mole ($H_2O$: $Li^+$) ratio, (b) viscosity, (c) electrical conductivity, (d) pH, and (e) temperature change after mixing of the lithium salts.

At a concentration of 1 m, all the electrolytes exhibit similar viscosity close to "water" approximately 1 cP(Joy & Wolfenden, 1930). The viscosity increases linearly at low concentrations, following Sprung's observations(Jones & Talley, 1933). However, when a higher amount of salt is added, the viscosity can increase significantly. This behavior agreed with the Arrhenius approximation ($\eta = A^c$), where $A$ is an empirical constant specific to each salt, and $c$ represents the concentration(Jones & Talley, 1933). Notably, the viscosity can be increase up to 13.67 ± 0.07 cP for a 20 m LiCl, 4.51 ± 0.07 cP for 15 m LiBr, 1.94 ± 0.01 cP for 10 m LiI, 2.72 ± 0.04 cP for 3 m $Li_2SO_4$, and 34.18 ± 1.58 cP for 20 m LiTFSI (at "water-in-salt" regime or maximum solubility). It is worth noting that increasing the salt concentration can enhance the energy density of energy storage through voltage expansion(Suo et al., 2015). However, it may also hinder electrolyte transport, limiting power density(Iamprasertkun et al., 2020; Lannelongue et al., 2018). Among all the electrolytes, $LiNO_3$ maintains a consistent viscosity of around 4.89 ± 0.06 cP, even when the concentration is increased to 20 m. The viscosity level of $LiNO_3$ is also similar to that of LiBr and LiI at the lower concentrations. Besides, the LiTFSI electrolyte show high viscosity when compared with other lithium-based salts at the same electrolyte concentration. This limits the specific power when apply LiTFSI as electrolyte in energy storage. Apart from the viscosity, it can be seen that the ionic conductivity of the electrolytes (Figure 4.5c) was increased when applied higher salt concentrations due to the surge of free ions; however, this phenomenon occurs as long as there are sufficient free space for cation and anion in the medium (water)(Q.-G. Zhang et al., 2011). When the electrolyte having more salts, the ionic conductivity decreases due to the ion pairing effects making the charge become close to one another(Fuoss, 1978). Thus, the hydration shell and the ionic association then play an importance role in the ionic conductivity(B. S. Krumgalz, 1982). At 20 m $LiNO_3$ exhibits a higher ionic conductivity (153.01 ± 0.26 mS $cm^{-1}$) than that of other salts. This is twice as high as 20 m LiCl, which was reported to be one of the alternative "water-in-salt(Bunpheng et

al., 2023), and almost 15 times higher than that of conventional “water-in-salt” electrolyte (20 m LiTFSI). Note that the highest conductivity of lithium halide family including LiCl, LiBr, and LiI were recorded at 5 m, and yet decreasing along the concentration, respectively. One common issue with many “water-in-salt electrolytes”(Dou, Lei, Wang, Zhang, Xiao, Guo, Wang, Yang, Li, & Shi, 2018; Suo et al., 2015), is that they tend to freeze and recrystallise at temperatures at below room temperature. This freezing can result in a decrease in conductivity. However, this is not the case for all superconcentrated electrolytes, as some, like $LiNO_3$, still maintain high electrical conductivity even at low temperatures(Amiri & Bélanger, 2021b).

Moreover, the pH of the electrolyte is sensitive to the concentration (see Figure 4.5d), this can represent the cell corrosion behavior with the metal substrate when applied to those salts. Only LiTFSI can maintain the pH as close to neutral condition when the concentration was increased. Therefore, this is one of advantages of using LiTFSI as an electrolyte, the corrosion is less concern in this case, especially the corrosion of aluminum substrate(Gabryelczyk, Ivanov, Bund, & Lota, 2021). The other salts e.g., LiBr, and LiI turned from basic to neutral after the concentration reached maximum. Besides, the $LiNO_3$, and LiCl exhibit almost neutral at the concentration of 1 m, however, those electrolytes were observed to be super acidic at “water-in-salt” concentration. Therefore, it is suggested that the anti-corrosion substrate should be apply when using halide and nitrate based electrolytes(Chomkhuntod et al., 2021). Deng *et al.*, investigated the acidity of hydrated lithium cations in organic solutions. Their hypothesis is the deprotonation process of water molecules losing protons directly linked to lithium ions and a redistribution of protons within the surrounding solvation shell(Critchfield & Johnson, 1959). This discovery carries significant implications for understanding the increased potential window and ionic mobility of “water-in-salt”(Deng et al., 2014).

Moreover, mixing the electrolyte definitely cause heat of mixing(Wood & Smith, 1965); thus, the record of temperature change during mixing is also crucial for the preparation of the electrolyte in large scale. Figure 4.5e shows the temperature change ($\Delta T$) after mixing those lithium-based electrolytes from “salt-in-water” to “water-in-salt”. It is found that the lithium halide-based electrolytes including lithium sulphate show an exothermic process during mixing where the temperature increased

up to 327, 327, 336 and 279 K for LiCl, LiBr, LiI, and $Li_2SO_4$ (at maximum conditions), respectively. In contrast, the LiTFSI and $LiNO_3$ show an endothermic, which consume the heat from surrounding during mixing. There is less effect of the heat of mixing for both LiTFSI and $LiNO_3$ when preparing a high concentration electrolyte ($\Delta T$ < 10 K).

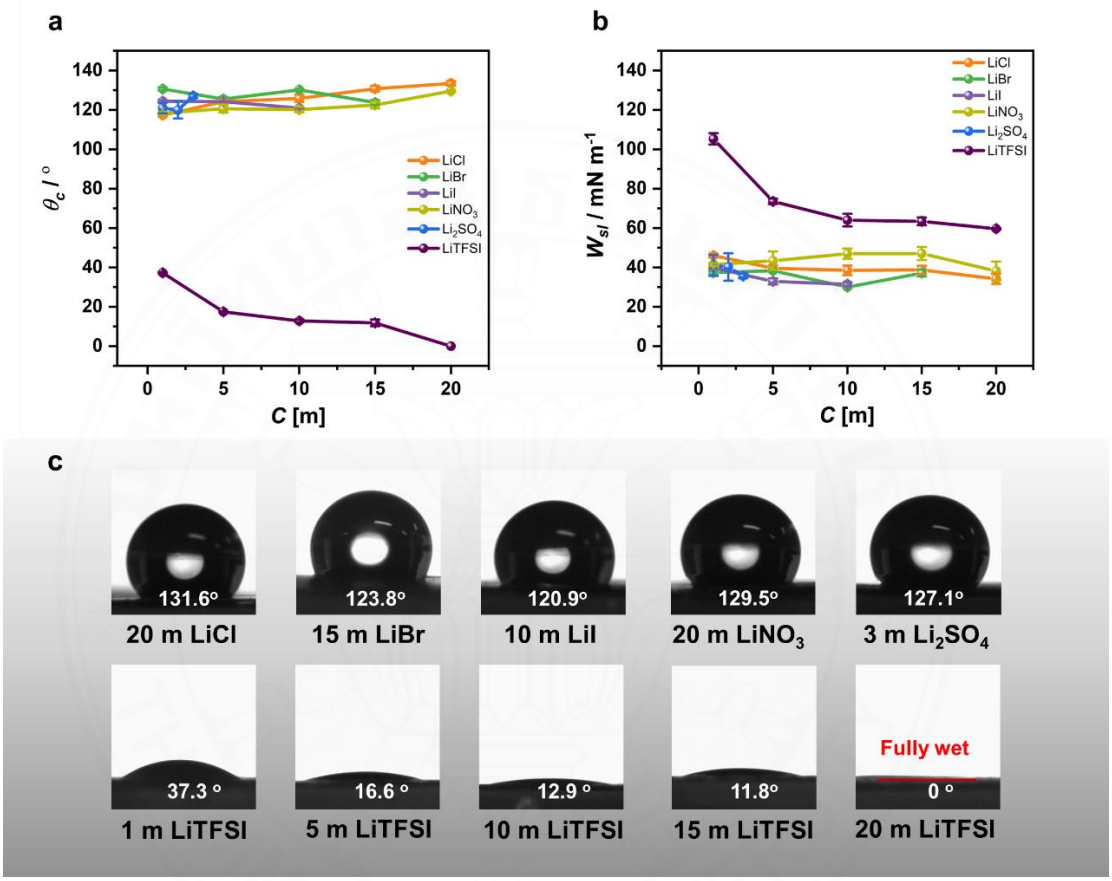


**Figure 4.6** The surface tension and contact angle measurement of lithium-based electrolytes with respect to the electrolyte concentration: (a) surface tension, (b) work of adhesion, and (c) contact angle at highest concentration of electrolyte (top) and the contact angle of LiTFSI from 1 m to 20 m.

In addition to the physical properties of various lithium-based electrolytes, the wettability characteristics including tension of electrolytes are demonstrated in Figure 13 Overall, the shift in wettability can be attributed to the alteration of interfacial tension between the liquid and air (as shown in Figure 4.6a). The liquid-air tension can both increase and decrease after the salts were introduced to deionised water. This is agreed with the observation of Yizhak Marcus work, he has point out that Hofmeister

series of ions(Boström, Kunz, & Ninham, 2005) is not always followed by the ionic surface tension increment(Marcus, 2010). Therefore, it is important to explore the wettability and tension of the specific electrolytes after the concentration has increased to “water-in-salt”. Surface tension can be described as a gauge of the appealing forces existing among the molecules positioned on the surface of a liquid. The reason that pure water exhibits relatively elevated surface tension is the result of robust hydrogen bonding between water molecules. Upon the addition of most salts, it promptly dissociates into cations and anions, resulting in a considerably more pronounced attraction of water molecules surrounding these ions, a phenomenon known as hydration. The H- ends of water molecules align themselves around the negatively charged anions, while the O ends similarly arrange themselves around cations(B Kronberg, K Holmberg, & B Lindman, 2014)·(Al-Zaidi & Fan, 2018). This enhanced hydration effect leads to an overall increase in the attractive forces between these hydrated, charged species as more salt is introduced, thereby causing a concurrent increase in surface tension(Vinš, Hykl, & Hrubý, 2019). On the other hand, the surface tension of water declined once LITFSI was introduced to water. This is due to the TFSI anions are absorbed to water surface, showing surfactant behavior(Groves, Perez-Martinez, Lhermerout, & Perkin, 2021; Y. Zhang et al., 2021). The change of surface tension directly affects the wettability on the surface; thus, the work of adhesion (Figure 4.6b) is then calculated to describe how the water attached to the activated carbon surfaces. It is found that electrolytes such as LiCl, LiBr, LiI, $LiNO_3$, and $Li_2SO_4$ exhibit work of adhesion ranging from 30.0 ± 0.5 mN $m^{-1}$ to 47.0 ± 3.3 mN $m^{-1}$, indicating relatively low adhesion to the electrode surface. These findings suggest that the electrolytes do not wet the electrode surface effectively due to stronger cohesive forces relative to adhesive forces. Hence, salts such as LiCl (131.6º ± 1.8), LiBr (123.8º ± 1.4), LiI (120.9º ± 0.2), $LiNO_3$ (129.5º ± 0.6), and $Li_2SO_4$ (127.1º ± 1.3) are notably superhydrophobic (see Figure 4.6c), especially at “water-in-salt” conditions. This highlights the importance of utilizing salts as "water-in-salt" electrolytes and underscores the need for fine-tuning wettability within this electrolyte family e.g., the development of hydrophilic surfaces are required(Amiri & Bélanger, 2021a; Deerattrakul et al., 2023). In contrast, the LiTFSI exhibits higher separation energies ranging from 59.6 ± 0.5 mN $m^{-1}$ to 105.3 ± 3.5 mN $m^{-1}$, showing hydrophilic properties

on the carbon surface. The LiTFSI electrolyte from 1 m to 20 m provide contact angle of 37.3º ± 0.4, 16.6º ± 1.8, 12.9º ± 0.9, 11.8º ± 2.1 and 0º, respectively. Therefore, the more concentrated of LITFSI electrolyte can provide a higher degree of wettability (a fully wet state is then found at 20 m LiTFSI). Note that the additional experiments including data Table 4.2.

**Table 4.2** Show the surface tension and wettability of electrolytes properties of a lithium electrolyte based on the expected concentration (m).

| Electrolytes | Concentration (m) | Wettability ($^{O}$) | Surface tension ($\gamma$) | Work of adhesion (mN $m^{-1}$) |
|---|---|---|---|---|
| **LiCl** | 1 | 117.3 ± 0.9 | 85.07 ± 0.06 | 46.01 ± 1.21 |
| | 5 | 124.2 ± 1.2 | 90.28 ± 3.42 | 39.58 ± 1.88 |
| | 10 | 125.8 ± 2.3 | 92.87± 0.09 | 38.53 ± 3.03 |
| | 15 | 131.5 ± 1.6 | 111.58 ± 0.15 | 37.61 ± 2.33 |
| | 20 | 131.6 ± 1.8 | 109.51 ± 4.07 | 36.80 ± 3.23 |
| **LIBr** | 1 | 130.6 ± 1.0 | 107.20 ± 2.29 | 37.38 ± 1.05 |
| | 5 | 125.5 ± 1.3 | 91.41 ± 3.06 | 38.30 ± 0.74 |
| | 10 | 130.2 ± 0.6 | 84.72 ± 2.64 | 30.03 ± 0.54 |
| | 15 | 123.8 ± 1.4 | 83.52 ± 2.52 | 37.11 ± 2.11 |
| **LiI** | 1 | 124.4 ± 0.8 | 91.61 ± 3.77 | 39.83 ± 0.68 |
| | 5 | 124.2 ± 0.3 | 75.07 ± 4.25 | 32.91 ± 1.91 |
| | 10 | 120.9 ± 0.2 | 64.63 ± 2.50 | 31.44 ± 1.22 |
| **$LiNO_3$** | 1 | 118.4 ± 0.6 | 79.19 ± 0.28 | 41.49 ± 0.74 |
| | 5 | 120.6 ± 2.3 | 88.27 ± 5.91 | 43.40 ± 4.68 |
| | 10 | 120.2 ± 1.7 | 94.49 ± 6.43 | 46.95 ± 2.63 |
| | 15 | 122.5 ± 2.1 | 101.67 ± 5.59 | 47.03 ± 3.33 |
| | 20 | 129.5 ± 0.6 | 105.25 ± 14.89 | 38.20 ± 4.76 |
| **$Li_2SO_4$** | 1 | 121.0 ± 3.4 | 84.03 ± 4.75 | 41.00 ± 6.50 |
| | 2 | 119.9 ± 5.3 | 79.69 ± 4.81 | 40.22 ± 8.52 |
| | 3 | 127.1 ± 1.3 | 89.92 ± 1.20 | 35.68 ± 1.42 |
| **LiTFSI** | 1 | 37.3 ± 0.4 | 58.64 ± 1.80 | 105.31 ± 3.48 |
| | 5 | 16.6 ± 1.8 | 37.64 ± 0.86 | 73.71 ± 1.40 |
| | 10 | 12.9 ± 0.9 | 32.42 ± 2.02 | 64.02 ± 3.94 |

| | | | |
|---|---|---|---|
| 15 | 11.8 ± 2.1 | 32.05 ± 1.34 | 63.40 ± 2.42 |
| 20 | 0.0 | 29.81 ± 0.23 | 59.63 ± 0.47 |

### 4.2.2 Electrochemistry Properties

The electrochemistry of the "salts-in-water" and "water-in-salts" are shown in Figure 4.7a When performing the electrochemistry of those prepared electrolytes on an activated carbon coated on glassy carbon electrode, most of the CVs were expanded after the electrolyte concentration was increased to "water-in-salt" regimes except for LiCl, LiBr and LiI. This is due to those species that can provide redox properties when applying the potential to the electrode surface. It is found that LiCl LiBr and LiI in super concentrations ("salt-in-water" and "water-in-salt") display a voltage window from -1.0 to 1.0 V vs. Ag/AgCl. The resault 20 m LiCl, the reduction peak take place at 1.23 V vs. Ag/AgCl. For 15 m LiBr, The yellow color belonging to bromine gas ($Br_2$) are present at the interfaces due to the reduction of $Br^-$ species(Kwak et al., 2016) the bromine reduction peak takes place at 0.56 V vs. Ag/AgCl(Kwak et al., 2016) while the onset was shifted to 0.57 V vs. Ag/AgCl when the superconcentrated solution was applied. Again, the result of 10 m LiI shows that the electrolyte solution turn into yellow color, due to the oxidation and reduction of iodide to iodine, which takes place at 0.24 V vs. Ag/AgCl(Wietelmann & Bauer, 2000). It has been proposed that the elevated overpotential observed during the reduction peak is attributed to the presence of non-electroactive layers of absorbed halide ions(Hanson, Matlosz, Tobias, & Newman, 1987). Therefore, it is suggested that the increase of concentrations in the redox salts (e.g., LiCl, LiBr, and LiI) can improve the redox reaction (oxidation/reduction), which the reaction can occur faster than that of lower concentration, even though the voltage window remains unchanged. Kwak *et.al.* have demonstrated that LiBr can be used as redox mediator coupled with the supporting electrolytes e.g. LiTFSI(Kwak et al., 2016). Therefore, it can be concluded that the LiBr and LiI either low or high concentration are not suitable for being a pure "water-in-salt" electrolyte. However, those two salts can be used as redox additive when coupling the electrolyte forming "water-in-bisalt"(Forero-Saboya, Hosseini-Bab-Anari, Abdelhamid, Moth-Poulsen, & Johansson, 2019). For LiCl, the voltage window expands *ca.* 0.3 V after the concentration turns into "water-in-salt" at 20 m. However, the corrosion of this

electrolyte is undeniable, alternative substrate or corrosion protection techniques must be applied to avoid the corrosion of substrate(Deerattrakul et al., 2023). Interestingly, 20 m $LiNO_3$ achieved 2.0 V for superconcentration. The extended voltage can be described by the diminishment of water shells, which are surrounded by Li-ion(Iamprasertkun et al., 2020; Suo et al., 2015). Zheng *et.al.*, showed that increasing $LiNO_3$ contents could alter the structure of hydrated Li-ion (typically, blinded with 4 water molecules) to $Li^+(H_2O)_4$ complex, and $(Li^+(H_2O)_2)_n$ polymer-like aggregation at 20 m(Zheng et al., 2018). This makes superconcentrated $LiNO_3$ become high voltage electrolyte, which is comparable to LiTFSI. Remarks, the CVs of LiTFSI achieved 2.44 V vs. Ag/AgCl in our system. For the $Li_2SO_4$, the gas evolution reaction may not be found in $Li_2SO_4$ cases, however, $Li_2SO_4$ provides too large *iR* drops, which is not possible to use as energy storage electrolyte. The electrode modification is needed for solving this issue(Oliveira et al., 2020).

Apart from voltage window, the specific capacitance in each electrolyte is also important to build high energy density devices. Figure 4.7b presents that the LiTFSI exhibits highest specific capacitance (208.23 F $g^{-1}$ at 10 mV $s^{-1}$), the capacitance decay is found to be around 68 percent when the scan rate was increased ten times (66.09 F $g^{-1}$, 100 mV $s^{-1}$). When observing the trend within the lithium halide group, it is found that the specific capacitances can be sorted in the order LiCl (18.48 F $g^{-1}$) < LiBr (121.15 F $g^{-1}$) < LiI (191.73 F $g^{-1}$), the capacitance were quoted at 10 mV $s^{-1}$. Moreover, the capacitance of $LiNO_3$ and $LiSO_4$ are reported to be 40.04 F $g^{-1}$, and 77.29 F $g^{-1}$ (10 mV $s^{-1}$), respectively.

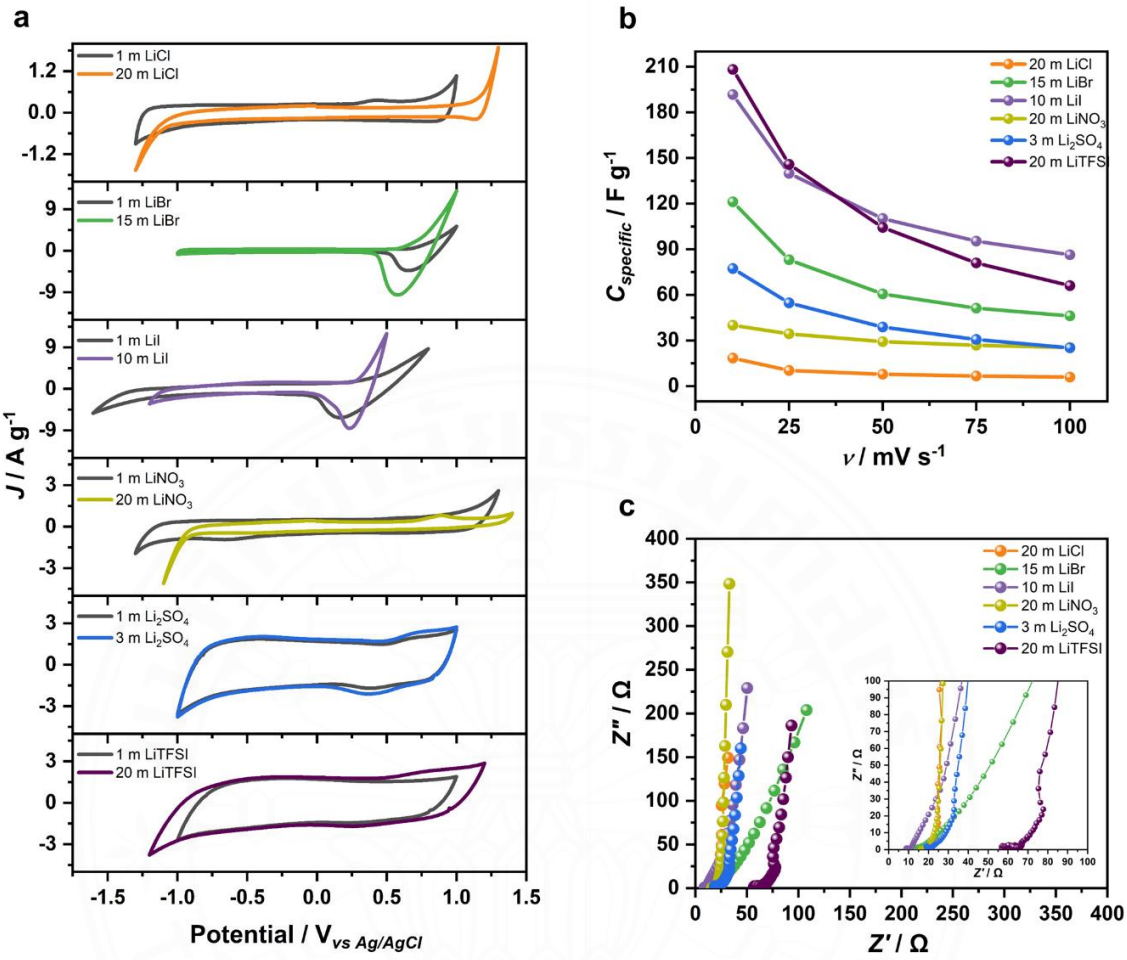


**Figure 4.7** The electrochemical properties of activated carbon electrode (three electrode configuration) in a specific electrolyte compared at 1 m and maximum concentration (a) CVs at 10 mV $s^{-1}$, (b) specific capacitance with respect to scan rates, and (c) Nyquist plots of difference electrolytes for a various electrolyte at superconcentration in three electrode system (AC-coated on glassy carbon electrode).

The electrochemical impedance spectroscopy (EIS) technique was used to study the electrical properties, contribution of electrode or electrolytic in electrochemical systems (Ribeiro & Abrantes, 2016). The electrochemical impedance spectroscopy is performed and represented in the internal resistance of the cells; the corresponding Nyquist plots of the electrolytes at 25 $^{o}$C are shown in Figure 4.7c. Lithium halide family exhibit small semicircle, indicating more efficient electrolyte ion diffusion due to the low charge transfer resistance when compared with the LiTFSI electrolyte. While LiCl exhibits the most deviation

line to the vertical axis, indicating poor capacitive behaviour, which are in good agreement with all results. The $R_{int}$ (internal resistance) of LiCl, LiBr, LiI, $LiNO_3$, $Li_2SO_4$ and LiTFSI are 22.26, 12.28, 10.53, 25.37, 20.09 and 33.19 Ω respectively.

To demonstrate the properties of those electrolytes in the device scale (demonstrated with symmetrical supercapacitors), the electrochemical performance of carbon-based supercapacitors in various "water-in-salt" electrolytes are shown in Figure 4.8. Note that YEC-8A with a specific surface area of 1,955 $m^2 g^{-1}$, and average pore size of 0.81 nm was used as active materials, which was coated on aluminium substrate. The mass loading of the activated carbon including conductive additive and binder was 11.09 ± 1.08 mg $cm^{-2}$ (carbon black and PVDF were used as additives at the ratio of 85:5:10). The electrochemical performance of the as-fabricated supercapacitors was further studied using cyclic voltammetry (CV), galvanostatic charge-discharge (GCD), and electrochemical impedance spectroscopy (EIS) in a symmetrical coin cell with superconcentration electrolytes.

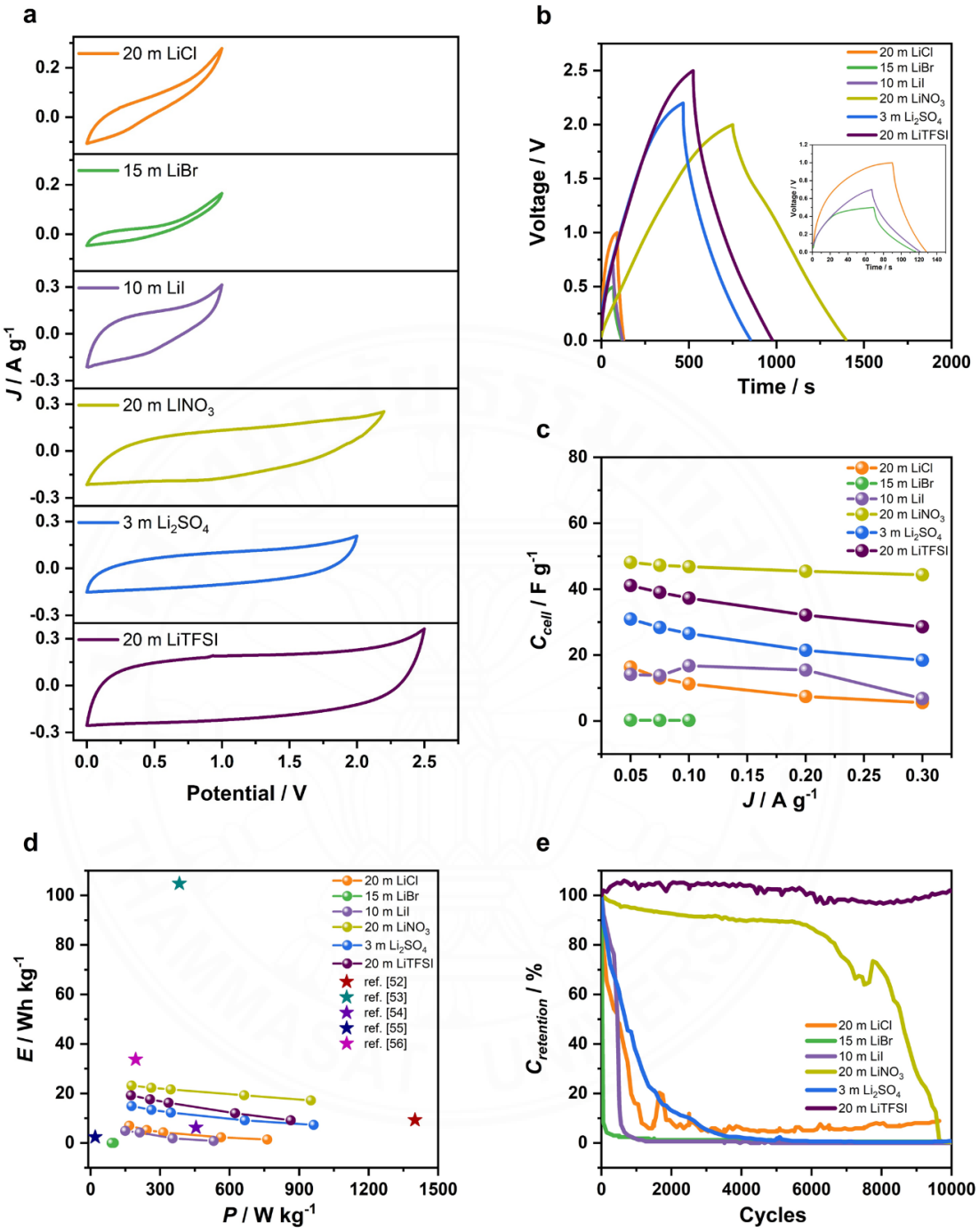


**Figure 4.8** The electrochemical performances of supercapacitors using superconcentration electrolytes of the symmetric cell: (a) CV curves at 10 mV $s^{-1}$. (b) GCD curve at maximum voltage with a current density of 0.1 A $g^{-1}$, (c) Cell capacitance with respect to current density (A $g^{-1}$), (d) Ragone plot, and(e) cycling stability at a current density of 0.1 A $g^{-1}$

Overall, the CVs in Figure 4.8a were operated at capacitive regions in order to ensure that there is no gas evolution occur in the system. We then catagorised the electrolyte into three main groups: (i) halide based (top), (ii) -ate based i.e., oxygen containing anion (middle), and (iii) TFSI (bottom). For the halide based, it is found that the voltage window is narrow unlike three electrode measurements, only 0.42 V, 0.43 V, and 0.62 V for LiCl, LiBr, and LiI, respectively. Applying large window can cause the gas evolution due to the anion e.g., $Br_2$, and $I_2$, this includes the corrosion of the substrate. It is suggested that the supporting electrolytes are required for those mentioned salts, forming either deep eutectic electrolytes(Di Pietro et al., 2022; Puttaswamy, Mondal, Mondal, & Ghosh, 2022) or redox electrolytes(Qin et al., 2020). For oxygen containing anion (-ate), it exhibits almost similar voltage as measured in three electrode configurations. $LiNO_3$ and $Li_2SO_4$ provide voltage window of 1.61 V and 1.64 V with a rectangular like shape CVs, respectively. However, it is noted that the $Li_2SO_4$ exhibits large *iR* drop as display in Figure 4.8b The GCDs in for a comparison, the LiTFSI was scanned from 0.0 V to 1.0 V (typical reported voltage window) (Suo et al., 2015). However, the GCD shows that the LiTFSI achieved approximately 2.5 V for our case, this is in good agreement with the voltage reported using three electrode configurations. Apart from voltage, the capacitance is also crucial for evaluating the specific energy of the supercapacitors. It is obvious that 20 m $LiNO_3$ demonstrated highest cell capacitance of 46.84 F $g^{-1}$ at current density 0.1 A $g^{-1}$ (see Figure 4.8c). Besides, 20 m LiTFSI shows the capacitance 37.28 F $g^{-1}$, 3 m $Li_2SO_4$ is 26.56 F $g^{-1}$, 10 m LiI is 16.77 F $g^{-1}$, and 20 m LiCl is 11.30 F $g^{-1}$. The 15 m LiBr electrolyte exhibits lowest capacitance of 0.29, 0.20, and 0.23 F $g^{-1}$ (0.05 A $g^{-1}$ to 0.1 A $g^{-1}$), respectively.

In addition to the CVs and GCDs, Figure 4.8d shows the comparison of gravimetric energy and power densities of the as-assembled coin cell using different superconcentrated electrolytes. The LiTFSI is the ideal candidate showing energy density up to 19.23 Wh $kg^{-1}$ (power density of 174.09 W $kg^{-1}$). Besides, $LiNO_3$ provides the higher energy density and power density of 17.19 Wh $kg^{-1}$ and 950.724 W $kg^{-1}$ among all “water-in-salt” electrolytes. The electrochemical performance of the as-fabricated supercapacitors is summarised in Table 4.3 including the benchmark of other electrolytes (literatures) using activated carbon YEC-8A. Therefore, it is concluded that

the LiTFSI is suitable for high energy applications while $LiNO_3$ is more suitable for high power applications. Testing involving 10,000 charging and discharging cycles at 0.1 A $g^{-1}$, the LiTFSI electrolyte supercapacitor demonstrated outstanding cycling stability with retention throughout the cycles. Remarkably, $LiNO_3$ exhibits intriguing results, However, this performance surpassed the retention levels observed in $Li_2SO_4$, LiCl, LiI, and LiBr electrolyte supercapacitors, as shown in Figure 4.8e. The compelling electrochemical properties exhibited by this electrolyte position it as an appealing choice for the fabrication of the next generation of supercapacitors, emphasizing its potential for advancing energy storage technologies.

**Table 4.3** The performance comparison of YEC-8A supercapacitor fabricated with superconcentrated electrolytes among different lithium-based salts in coin cell level (evaluated from 0.05 A $g^{-1}$ to 0.3 A $g^{-1}$).

| **Electrolytes** | ***ΔV* (V)** | ***C*$_{cell}$ (F g$^{-1}$)** | ***E* (Wh kg$^{-1}$)** | ***P* (W kg$^{-1}$)** |
|---|---|---|---|---|
| 20m LiCl | 0.87 | 11.30 | 1.39 - 7.00 | 166.57 - 762.26 |
| 15 m LiBr | 0.25 | 0.23 | 0.01 - 0.04 | 91.08 - 100.09 |
| 10 m LiI | 0.75 | 16.77 | 0.82 - 4.89 | 149.65 - 531.14 |
| 20 m $LiNO_3$ | 0.96 | 46.84 | 17.19 - 23.20 | 176.71 - 950.72 |
| 3 m $Li_2SO_4$ | 0.96 | 26.56 | 7.82 - 14.92 | 176.76 - 962.60 |
| 20 m LITFSI | 0.93 | 37.29 | 9.14 - 19.23 | 174.09 - 863.67 |
| *21 m LiTFSI | - | - | 15 | 700 |
| **2 M $ZnSO_4$ | - | - | 104.8 | 383.5 |
| ***6 m KOH electrolyte | - | - | 6.27 | 455.17 |
| ****polymer gel electrolyte | - | 30 | 2.39 | 19.79 |
| *****0.5 M KCl | - | - | 33.75 | 194.4 |

*Reference [(Mahankali, Thangavel, Ding, Putatunda, & Arava, 2019)], **Reference [(Yang, Bissett, & Dryfe, 2021)], ***Reference [(K. Zhang et al., 2022)]****Reference[(Liew, Ramesh, & Arof, 2014)] and *****Reference[(Husmann, Zarbin, & Dryfe, 2020)].

### 4.2.3 The commercialisation of "water-in-salts" electrolytes

In addition to all scientific data, the commercialisation of "water-in-salts" electrolytes still faces challenges due to the need of a large amount of salt for maintaining voltage window of the electrolyte(Tian, Zhu, & Xu, 2021). Hence, the cost evaluation per unit of energy and power density was then summarised based on the price of commercial salts (AR-grade, Sigma-Aldrich).

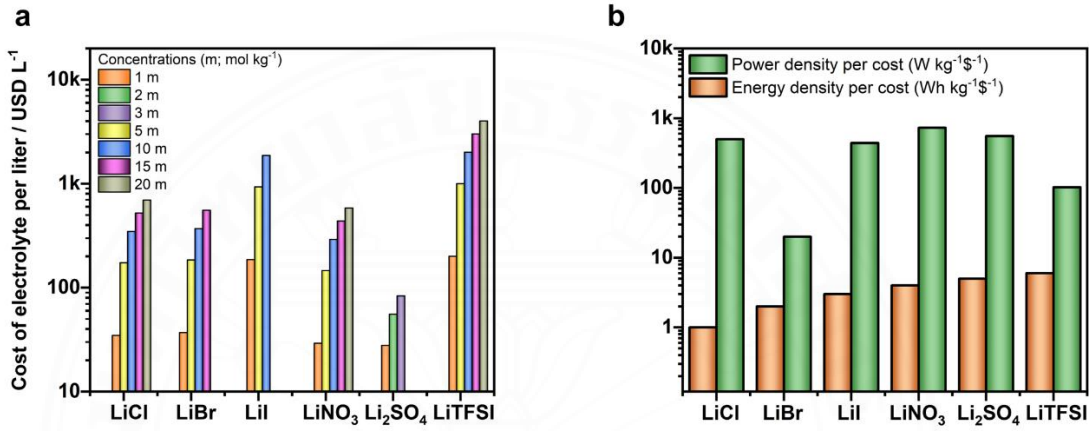


**Figure 4.9** Economic information of (a) cost of electrolytes based on the price of commercial salts (AR-grade) in Sigma-Aldrich at a variety of concentration, and (b) the normalised cost per unit of energy and power densities (1.0 V) gained.

It can be seen in Figure 4.9a that most of the common salts (LiCl, LiBr, $LiNO_3$, and $Li_2SO_4$) exhibit a low cost below one thousand dollas per liter of the superconcentrated electrolytes. Besides, LiI and LiTFSI shows extreamly high cost for superconcentration conditions (about 1867.20 to 4016.24 USD per liter). However, it should be noted that each salt has its own unique properties that make it suitable for a different applications, but the cost of the salt can impact its feasibility for being commercial use. For an energy storage perspective, Figure 4.9b shows the comparison of the energy/power density per cost of electrolytes, by comparing the energy and power density obtain from the prepared electrolytes. The traditional salts (e.g. LiCl, LiBr, LiI, $Li_2SO_4$, and $LiNO_3$) are more worth than that of LiTFSI electrolyte when considering the high power density applications. While less worth than that of LiTFSI when considering the energy

density. The “water-in-$LiNO_3$” provide highest power per cost of electrolyte, while LiTFSI is the winner of the energy.

# CHAPTER 5
# CONCLUSION

In a comprehensive survey of electrolyte properties Researchers have specifically studied lithium chloride (LiCl) electrolytes, from dilute solutions to "water-in-salt" formulations. These investigations have been extended to various carbon model systems. Including glassy carbon, graphite, and activated carbon. Lithium chloride has shown potential as a "water-in-salt" electrolyte, with a voltage range comparable to traditional electrolytes such as lithium bis (Trifluoromethanesulfonyl)imide This disclosure makes lithium chloride a possible alternative in aqueous-salt electrolytes. This is despite the use of graphite coated aluminum foil to reduce electrode corrosion in envelope cell devices.

The study also demonstrated the benefits of a 20 m lithium chloride solution in a pouch cell supercapacitor. This provides outstanding benchmark results of 1.6 V and 2.4 F $g^{-1}$ in terms of cell capacitance. This breakthrough underscores the emergence of lithium chloride as a potential option for advanced energy storage applications of "water-in-salt" electrolytes. on the other side Analysis of various lithium salt (LiX) electrolytes. From "salt in water" to "water in salt" configurations, it provides a wide range of insights. While lithium halide-based salts exhibit accelerated redox processes when shifted to “water-in-salt” concentrations, they fail to increase the voltage window at the device level. For this reason, these salts have found utility as redox additives. This facilitates the formation of electrolytes. Meanwhile Electrolytes containing oxygen-containing anions such as sulfates and nitrates. Shows outstanding characteristics Although both have a wide operating voltage range of 2.2 V, $Li_2SO_4$ shows a significant iR decrease during discharge. This requires surface modification to increase performance. $LiNO_3$, on the other hand, shows superior energy density characteristics. This is in contrast to LiTFSI which focuses on energy density.

This comprehensive analysis outlines the advantages and limitations of each electrolyte system. It emphasizes the importance of matching electrolyte properties to a specific electrochemical system to optimize device performance. This helps bridge the gap between laboratory research and commercial applications. This study gives us

a better understanding of the properties of electrolytes. It provides the basis for informed electrolyte selection and advancements in larger-scale energy storage technologies.

# REFERENCES

Akgul, E. T., Üzdürmez, A. F., Kamış, H., Kılıç, E., & Demir, M. (2021). Electrochemical preparation of donor-acceptor type conjugated polymer films: Effect of substitute units on electrochromic performance. *Optical Materials, 111*, 110635.

Al-Zaidi, E., & Fan, X. (2018). Effect of aqueous electrolyte concentration and valency on contact angle on flat glass surfaces and inside capillary glass tubes. *Colloids and Surfaces A: Physicochemical and Engineering Aspects, 543*, 1-8.

Albrecht, T., Gibb, T., & Nuttall, P. (2013). Chapter 1 - Ion Transport in Nanopores. In J. B. Edel & T. Albrecht (Eds.), *Engineered Nanopores for Bioanalytical Applications* (pp. 1-30). Oxford: William Andrew Publishing.

Ali, G. A. (2020). Recycled MnO2 nanoflowers and graphene nanosheets for low-cost and high performance asymmetric supercapacitor. *Journal of Electronic Materials, 49*(9), 5411-5421.

Amiri, M., & Bélanger, D. (2021a). Physicochemical and Electrochemical Properties of Water-in-Salt Electrolytes. *ChemSusChem, 14*(12), 2487-2500. doi:https://doi.org/10.1002/cssc.202100550

Amiri, M., & Bélanger, D. (2021b). Physicochemical and Electrochemical Properties of Water-in-Salt Electrolytes. *ChemSusChem, 14*(12), 2487-2500.

Armand, M. (1991). Process for synthesis of sulfonylimides. In: Google Patents.

Bhoyate, S., Ranaweera, C. K., Zhang, C., Morey, T., Hyatt, M., Kahol, P. K., . . . Gupta, R. K. (2017). Eco-Friendly and High Performance Supercapacitors for Elevated Temperature Applications Using Recycled Tea Leaves. *Global Challenges, 1*(8), 1700063. doi:https://doi.org/10.1002/gch2.201700063

Boström, M., Kunz, W., & Ninham, B. W. (2005). Hofmeister Effects in Surface Tension of Aqueous Electrolyte Solution. *Langmuir, 21*(6), 2619-2623. doi:10.1021/la047437v

Bouchet, R., Maria, S., Meziane, R., Aboulaich, A., Lienafa, L., Bonnet, J.-P., . . . Devaux, D. (2013). Single-ion BAB triblock copolymers as highly efficient electrolytes for lithium-metal batteries. *Nature materials, 12*(5), 452-457.

Bunpheng, A., Sakulaue, P., Hirunpinyopas, W., Nueangnoraj, K., Luanwuthi, S., & Iamprasertkun, P. (2023). Revisiting the properties of lithium chloride as "water-in-salt" electrolyte for pouch cell electrochemical capacitors. *Journal of Electroanalytical Chemistry, 944*, 117645. doi:https://doi.org/10.1016/j.jelechem.2023.117645

C. da Silva, D. A., Pinzón C, M. J., Messias, A., Fileti, E. E., Pascon, A., Franco, D. V., . . . Zanin, H. G. (2022). Effect of conductivity, viscosity, and density of water-in-salt electrolytes on the electrochemical behavior of supercapacitors: molecular dynamics simulations and in situ characterization studies. *Materials Advances, 3*(1), 611-623. doi:10.1039/D1MA00890K

Chen, M., Feng, G., & Qiao, R. (2020). Water-in-salt electrolytes: An interfacial perspective. *Current opinion in colloid & interface science, 47*, 99-110.

Chomkhuntod, P., Iamprasertkun, P., Chiochan, P., Suktha, P., & Sawangphruk, M. (2021). Scalable 18,650 aqueous-based supercapacitors using hydrophobicity concept of anti-corrosion graphite passivation layer. *Scientific Reports, 11*(1), 13082. doi:10.1038/s41598-021-92597-y

Choudhary, N., Li, C., Moore, J., Nagaiah, N., Zhai, L., Jung, Y., & Thomas, J. (2017). Asymmetric supercapacitor electrodes and devices. *Advanced Materials, 29*(21), 1605336.

Coustan, L., Shul, G., & Bélanger, D. (2017). Electrochemical behavior of platinum, gold and glassy carbon electrodes in water-in-salt electrolyte. *Electrochemistry Communications, 77*, 89-92. doi:https://doi.org/10.1016/j.elecom.2017.03.001

Critchfield, F., & Johnson, J. (1959). Effect of neutral salts on pH of acid solutions. *Analytical Chemistry, 31*(4), 570-572.

Daerr, A., & Mogne, A. (2016). Pendent_drop: an imagej plugin to measure the surface tension from an image of a pendent drop. *Journal of Open Research Software, 4*(1).

Deerattrakul, V., Sakulaue, P., Bunpheng, A., Kraithong, W., Pengsawang, A., Chakthranont, P., . . . Itthibenchapong, V. (2023). Introducing hydrophilic cellulose nanofiber as a bio-separator for "water-in-salt" based energy storage

devices. *Electrochimica Acta, 453*, 142355. doi:https://doi.org/10.1016/j.electacta.2023.142355

Deng, H., Peljo, P., Stockmann, T. J., Qiao, L., Vainikka, T., Kontturi, K., . . . Girault, H. H. (2014). Surprising acidity of hydrated lithium cations in organic solvents. *Chemical Communications, 50*(42), 5554-5557.

Di Pietro, M. E., Goloviznina, K., van den Bruinhorst, A., de Araujo Lima e Souza, G., Costa Gomes, M., Padua, A. A. H., & Mele, A. (2022). Lithium Salt Effects on the Liquid Structure of Choline Chloride–Urea Deep Eutectic Solvent. *ACS Sustainable Chemistry & Engineering, 10*(36), 11835-11845. doi:10.1021/acssuschemeng.2c02460

Dou, Q., Lei, S., Wang, D.-W., Zhang, Q., Xiao, D., Guo, H., . . . Shi, S. (2018). Safe and high-rate supercapacitors based on an "acetonitrile/water in salt" hybrid electrolyte. *Energy & Environmental Science, 11*(11), 3212-3219.

Dou, Q., Lei, S., Wang, D.-W., Zhang, Q., Xiao, D., Guo, H., . . . Yan, X. (2018). Safe and high-rate supercapacitors based on an "acetonitrile/water in salt" hybrid electrolyte. *Energy & Environmental Science, 11*(11), 3212-3219. doi:10.1039/C8EE01040D

Droguet, L., Grimaud, A., Fontaine, O., & Tarascon, J. M. (2020). Water-in-salt electrolyte (WiSE) for aqueous batteries: a long way to practicality. *Advanced Energy Materials, 10*(43), 2002440.

Eugene Huang, A. S., Terence Denning, Jianzhong Qi, Raymond R. Dagastine, Rico F. Tabor, Joseph D. Berry. (2021). OpenDrop: Open-source software for pendant drop tensiometry & contact angle measurements. *Journal of Open Source Software, 6*(58), 2604. doi:https://doi.org/10.21105/joss.02604

Forero-Saboya, J., Hosseini-Bab-Anari, E., Abdelhamid, M. E., Moth-Poulsen, K., & Johansson, P. (2019). Water-in-Bisalt Electrolyte with Record Salt Concentration and Widened Electrochemical Stability Window. *The Journal of Physical Chemistry Letters, 10*(17), 4942-4946. doi:10.1021/acs.jpclett.9b01467

Fuoss, R. M. (1978). Conductance-concentration function for the paired ion model. *The Journal of Physical Chemistry, 82*(22), 2427-2440. doi:10.1021/j100511a017

Gabryelczyk, A., Ivanov, S., Bund, A., & Lota, G. (2021). Corrosion of aluminium current collector in lithium-ion batteries: A review. *Journal of Energy Storage, 43*, 103226. doi:https://doi.org/10.1016/j.est.2021.103226

Gambou-Bosca, A., & Bélanger, D. (2016). Electrochemical characterization of MnO2-based composite in the presence of salt-in-water and water-in-salt electrolytes as electrode for electrochemical capacitors. *Journal of Power Sources, 326*, 595-603. doi:https://doi.org/10.1016/j.jpowsour.2016.04.088

Goldsack, D. E., & Franchetto, A. A. (1977). The viscosity of concentrated electrolyte solutions—III. A mixture law. *Electrochimica Acta, 22*(11), 1287-1294. doi:https://doi.org/10.1016/0013-4686(77)87012-6

Goldsack, D. E., & Franchetto, R. (1977). The viscosity of concentrated electrolyte solutions. I. Concentration dependence at fixed temperature. *Canadian Journal of Chemistry, 55*(6), 1062-1072. doi:10.1139/v77-148

Groves, T. S., Perez-Martinez, C. S., Lhermerout, R., & Perkin, S. (2021). Surface Forces and Structure in a Water-in-Salt Electrolyte. *The Journal of Physical Chemistry Letters, 12*(6), 1702-1707. doi:10.1021/acs.jpclett.0c03718

Hanson, K. J., Matlosz, M. J., Tobias, C. W., & Newman, J. (1987). Electrochemistry of Iodide in Propylene Carbonate: II. Theoretical Model. *Journal of the Electrochemical Society, 134*(9), 2210.

Hirunpinyopas, W., Iamprasertkun, P., Fevre, L. W. L., Panomsuwan, G., Sirisaksoontorn, W., Dryfe, R. A. W., & Songsasen, A. (2022). Insights into binding mechanisms of size-selected graphene binders for flexible and conductive porous carbon electrodes. *Electrochimica Acta, 403*, 139696. doi:https://doi.org/10.1016/j.electacta.2021.139696

Hirunpinyopas, W., Iamprasertkun, P., Le Fevre, L. W., Panomsuwan, G., Sirisaksoontorn, W., Dryfe, R. A., & Songsasen, A. (2022). Insights into binding mechanisms of size-selected graphene binders for flexible and conductive porous carbon electrodes. *Electrochimica Acta, 403*, 139696.

Huang, J., Yuan, K., & Chen, Y. (2022). Wide voltage aqueous asymmetric supercapacitors: advances, strategies, and challenges. *Advanced Functional Materials, 32*(4), 2108107.

Hunter, R. J., White, L. R., & Chan, D. Y. (1987). Foundations of colloid science. *(No Title)*.

Husmann, S., Zarbin, A. J., & Dryfe, R. A. (2020). High-performance aqueous rechargeable potassium batteries prepared via interfacial synthesis of a Prussian blue-carbon nanotube composite. *Electrochimica Acta, 349*, 136243.

Iamprasertkun, P., Ejigu, A., & Dryfe, R. A. W. (2020). Understanding the electrochemistry of "water-in-salt" electrolytes: basal plane highly ordered pyrolytic graphite as a model system. *Chemical Science, 11*(27), 6978-6989. doi:10.1039/D0SC01754J

Iamprasertkun, P., Hirunpinyopas, W., Deerattrakul, V., Sawangphruk, M., & Nualchimplee, C. (2021). Controlling the flake size of bifunctional 2D WSe2 nanosheets as flexible binders and supercapacitor materials. *Nanoscale Advances, 3*(3), 653-660. doi:10.1039/D0NA00592D

Inal, I. I. G., & Aktas, Z. (2020). Enhancing the performance of activated carbon based scalable supercapacitors by heat treatment. *Applied Surface Science, 514*, 145895.

Jiang, H., Yan, X., Miao, J., You, M., Zhu, Y., Pan, J., . . . Cheng, X. (2021). Super-conductive silver nanoparticles functioned three-dimensional CuxO foams as a high-pseudocapacitive electrode for flexible asymmetric supercapacitors. *Journal of Materiomics, 7*(1), 156-165.

Jones, G., & Talley, S. K. (1933). The Viscosity of Aqueous Solutions as a Function of the Concentration. *Journal of the American Chemical Society, 55*(2), 624-642. doi:10.1021/ja01329a024

Joy, W. E., & Wolfenden, J. H. (1930). Viscosity of Electrolytes. *Nature, 126*(3191), 994-995. doi:10.1038/126994b0

Karlsson, R. K. B., & Cornell, A. (2016). Selectivity between Oxygen and Chlorine Evolution in the Chlor-Alkali and Chlorate Processes. *Chemical Reviews, 116*(5), 2982-3028. doi:10.1021/acs.chemrev.5b00389

Kim, J. S., Wu, Z., Morrow, A. R., Yethiraj, A., & Yethiraj, A. (2012). Self-Diffusion and Viscosity in Electrolyte Solutions. *The Journal of Physical Chemistry B, 116*(39), 12007-12013. doi:10.1021/jp306847t

Kronberg, B., Holmberg, K., & Lindman, B. (2014). Surface and interfacial tension. *Kronberg B, Holmberg K, Lindman B. Surface chemistry of surfactants and polymers. Wiley, United Kingdom*, p231-249.

Kronberg, B., Holmberg, K., & Lindman, B. (2014). *Surface chemistry of surfactants and polymers*: John Wiley & Sons.

Krumgalz, B. (1974). Krumgalz, B.S. 1974. Interaction of tetraalkylammonium and some other organic ions with solvent molecules. J. Gen. Chem., 44: 1585-1588.

Krumgalz, B. S. (1982). Ion-solvent interactions and ionic association in ethanol solutions. *Journal of Solution Chemistry, 11*(4), 283-293. doi:10.1007/BF00657319

Kwak, W.-J., Hirshberg, D., Sharon, D., Afri, M., Frimer, A. A., Jung, H.-G., . . . Sun, Y.-K. (2016). Li–O2 cells with LiBr as an electrolyte and a redox mediator. *Energy & Environmental Science, 9*(7), 2334-2345. doi:10.1039/C6EE00700G

Lannelongue, P., Bouchal, R., Mourad, E., Bodin, C., Olarte, M., le Vot, S., . . . Fontaine, O. (2018). "Water-in-Salt" for Supercapacitors: A Compromise between Voltage, Power Density, Energy Density and Stability. *Journal of the Electrochemical Society, 165*(3), A657. doi:10.1149/2.0951803jes

Laschuk, N. O., Easton, E. B., & Zenkina, O. V. (2021). Reducing the resistance for the use of electrochemical impedance spectroscopy analysis in materials chemistry. *RSC Advances, 11*(45), 27925-27936. doi:10.1039/D1RA03785D

Le Fevre, L. W., Ejigu, A., Todd, R., Forsyth, A. J., & Dryfe, R. A. W. (2021). High temperature supercapacitors using water-in-salt electrolytes: stability above 100 °C. *Chemical Communications, 57*(43), 5294-5297. doi:10.1039/D1CC01087E

Liang, T., Hou, R., Dou, Q., Zhang, H., & Yan, X. (2021). The applications of water-in-salt electrolytes in electrochemical energy storage devices. *Advanced Functional Materials, 31*(3), 2006749.

Liew, C.-W., Ramesh, S., & Arof, A. K. (2014). Good prospect of ionic liquid based-poly (vinyl alcohol) polymer electrolytes for supercapacitors with excellent electrical, electrochemical and thermal properties. *International Journal of Hydrogen Energy, 39*(6), 2953-2963.

Lim, J. M., Jang, Y. S., Nguyen, H. V. T., Kim, J. S., Yoon, Y., Park, B. J., . . . Ostrikov, K. K. (2023). Advances in high-voltage supercapacitors for energy storage systems: materials and electrolyte tailoring to implementation. *Nanoscale Advances, 5*(3), 615-626.

Lim, T., Jung, G. Y., Kim, J. H., Park, S. O., Park, J., Kim, Y.-T., . . . Joo, S. H. (2020). Atomically dispersed Pt–N4 sites as efficient and selective electrocatalysts for the chlorine evolution reaction. *Nature Communications, 11*(1), 412. doi:10.1038/s41467-019-14272-1

Logan, E., Tonita, E. M., Gering, K., Li, J., Ma, X., Beaulieu, L., & Dahn, J. (2018). A study of the physical properties of Li-ion battery electrolytes containing esters. *Journal of the Electrochemical Society, 165*(2), A21.

Lu, Y., Tu, Z., Shu, J., & Archer, L. A. (2015). Stable lithium electrodeposition in salt-reinforced electrolytes. *Journal of Power Sources, 279*, 413-418.

Mahankali, K., Thangavel, N. K., Ding, Y., Putatunda, S. K., & Arava, L. M. R. (2019). Interfacial behavior of water-in-salt electrolytes at porous electrodes and its effect on supercapacitor performance. *Electrochimica Acta, 326*, 134989.

Marcus, Y. (2010). Surface Tension of Aqueous Electrolytes and Ions. *Journal of Chemical & Engineering Data, 55*(9), 3641-3644. doi:10.1021/je1002175

Matsumoto, K., Inoue, K., Nakahara, K., Yuge, R., Noguchi, T., & Utsugi, K. (2013). Suppression of aluminum corrosion by using high concentration LiTFSI electrolyte. *Journal of Power Sources, 231*, 234-238.

McCreery, R. L. (2008). Advanced Carbon Electrode Materials for Molecular Electrochemistry. *Chemical Reviews, 108*(7), 2646-2687. doi:10.1021/cr068076m

McEldrew, M., Goodwin, Z. A. H., Bi, S., Kornyshev, A. A., & Bazant, M. Z. (2021). Ion Clusters and Networks in Water-in-Salt Electrolytes. *Journal of The Electrochemical Society, 168*(5), 050514. doi:10.1149/1945-7111/abf975

Nguyen, H. V. T., Kim, J., & Lee, K.-K. (2021). High-voltage and intrinsically safe supercapacitors based on a trimethyl phosphate electrolyte. *Journal of Materials Chemistry A, 9*(36), 20725-20736.

Nualchimplee, C., Jitapunkul, K., Deerattrakul, V., Thaweechai, T., Sirisaksoontorn, W., Hirunpinyopas, W., & Iamprasertkun, P. (2022). Auto-oxidation of exfoliated MoS2 in N-methyl-2-pyrrolidone: from 2D nanosheets to 3D nanorods. *New Journal of Chemistry, 46*(2), 747-755. doi:10.1039/D1NJ05384A

Oliveira, R. D., Santos, C. S., Garcia, J. R., Vidotti, M., Marchesi, L. F., & Pessoa, C. A. (2020). IR drop studies of poly(aniline)-based modified electrodes. *Journal of Electroanalytical Chemistry, 878*, 114662. doi:https://doi.org/10.1016/j.jelechem.2020.114662

Pal, B., Yang, S., Ramesh, S., Thangadurai, V., & Jose, R. (2019). Electrolyte selection for supercapacitive devices: a critical review. *Nanoscale Advances, 1*(10), 3807-3835.

Park, J., Lee, J., & Kim, W. (2021). Water-in-Salt Electrolyte Enables Ultrafast Supercapacitors for AC Line Filtering. *ACS Energy Letters, 6*(2), 769-777. doi:10.1021/acsenergylett.0c02442

Puttaswamy, R., Mondal, C., Mondal, D., & Ghosh, D. (2022). An account on the deep eutectic solvents-based electrolytes for rechargeable batteries and supercapacitors. *Sustainable Materials and Technologies, 33*, e00477. doi:https://doi.org/10.1016/j.susmat.2022.e00477

Qin, W., Zhou, N., Wu, C., Xie, M., Sun, H., Guo, Y., & Pan, L. (2020). Mini-Review on the Redox Additives in Aqueous Electrolyte for High Performance Supercapacitors. *ACS Omega, 5*(8), 3801-3808. doi:10.1021/acsomega.9b04063

Ramachandran, T., Hamed, F., Raji, R. K., Majhi, S. M., Barik, D., Kumar, Y. A., . . . Ansar, S. (2023). Enhancing asymmetric supercapacitor performance with NiCo2O4–NiO hybrid electrode fabrication. *Journal of Physics and Chemistry of Solids, 180*, 111467.

Riaz, A., Sarker, M. R., Saad, M. H. M., & Mohamed, R. (2021). Review on comparison of different energy storage technologies used in micro-energy harvesting, WSNs, low-cost microelectronic devices: challenges and recommendations. *Sensors, 21*(15), 5041.

Ribeiro, D., & Abrantes, J. (2016). Application of electrochemical impedance spectroscopy (EIS) to monitor the corrosion of reinforced concrete: A new approach. *Construction and Building Materials, 111,* 98-104.

Ruschhaupt, P., Pohlmann, S., Varzi, A., & Passerini, S. (2020). Determining realistic electrochemical stability windows of electrolytes for electrical double-layer capacitors. *Batteries & Supercaps, 3*(8), 698-707.

Sajjad, M., Khan, M. I., Cheng, F., & Lu, W. (2021). A review on selection criteria of aqueous electrolytes performance evaluation for advanced asymmetric supercapacitors. *Journal of Energy Storage, 40,* 102729.

Sakamoto, R., Yamashita, M., Nakamoto, K., Zhou, Y., Yoshimoto, N., Fujii, K., . . . Okada, S. (2020). Local structure of a highly concentrated NaClO4 aqueous solution-type electrolyte for sodium ion batteries. *Physical Chemistry Chemical Physics, 22*(45), 26452-26458. doi:10.1039/D0CP04376A

Shabeeba, P., Thayyil, M. S., Pillai, M., Soufeena, P., & Niveditha, C. (2018). Electrochemical investigation of activated carbon electrode supercapacitors. *Russian Journal of Electrochemistry, 54,* 302-308.

Shao, Y., El-Kady, M. F., Sun, J., Li, Y., Zhang, Q., Zhu, M., . . . Kaner, R. B. (2018). Design and mechanisms of asymmetric supercapacitors. *Chemical reviews, 118*(18), 9233-9280.

Suo, L., Borodin, O., Gao, T., Olguin, M., Ho, J., Fan, X., . . . Xu, K. (2015). "Water-in-salt" electrolyte enables high-voltage aqueous lithium-ion chemistries. *Science, 350*(6263), 938-943. doi:10.1126/science.aab1595

Suo, L., Borodin, O., Sun, W., Fan, X., Yang, C., Wang, F., . . . Wang, C. (2016). Advanced High-Voltage Aqueous Lithium-Ion Battery Enabled by "Water-in-Bisalt" Electrolyte. *Angewandte Chemie International Edition, 55*(25), 7136-7141. doi:https://doi.org/10.1002/anie.201602397

Taberna, P., Simon, P., & Fauvarque, J.-F. (2003). Electrochemical characteristics and impedance spectroscopy studies of carbon-carbon supercapacitors. *Journal of the Electrochemical Society, 150*(3), A292.

Tian, X., Zhu, Q., & Xu, B. (2021). "Water-in-Salt" Electrolytes for Supercapacitors: A Review. *ChemSusChem, 14*(12), 2501-2515.

Uskoković, V. (2021). A historical review of glassy carbon: Synthesis, structure, properties and applications. *Carbon Trends, 5*, 100116. doi:https://doi.org/10.1016/j.cartre.2021.100116

Vinš, V., Hykl, J., & Hrubý, J. (2019). Surface tension of seawater at low temperatures including supercooled region down to – 25 °C. *Marine Chemistry, 213*, 13-23. doi:https://doi.org/10.1016/j.marchem.2019.05.001

Vos, J. G., Liu, Z., Speck, F. D., Perini, N., Fu, W., Cherevko, S., & Koper, M. T. M. (2019). Selectivity Trends Between Oxygen Evolution and Chlorine Evolution on Iridium-Based Double Perovskites in Acidic Media. *ACS Catalysis, 9*(9), 8561-8574. doi:10.1021/acscatal.9b01159

Wang, Y., Meng, X., Sun, J., Liu, Y., & Hou, L. (2020). Recent Progress in "Water-in-Salt" Electrolytes Toward Non-lithium Based Rechargeable Batteries. *Frontiers in Chemistry, 8*. Retrieved from https://www.frontiersin.org/article/10.3389/fchem.2020.00595

Widegren, J. A., & Magee, J. W. (2007). Density, viscosity, speed of sound, and electrolytic conductivity for the ionic liquid 1-hexyl-3-methylimidazolium bis (trifluoromethylsulfonyl) imide and its mixtures with water. *Journal of Chemical & Engineering Data, 52*(6), 2331-2338.

Wietelmann, U., & Bauer, R. J. (2000). Lithium and lithium compounds. *Ullmann's Encyclopedia of Industrial Chemistry*.

Wood, R. H., & Smith, R. W. (1965). Heats of Mixing of Aqueous Electrolytes. I. Concentration Dependence of 1-1 Electrolytes. *The Journal of Physical Chemistry, 69*(9), 2974-2979. doi:10.1021/j100893a025

Wu, F., Lee, J. T., Nitta, N., Kim, H., Borodin, O., & Yushin, G. (2014). Lithium iodide as a promising electrolyte additive for lithium-sulfur batteries: mechanisms of performance enhancement. *Advanced Materials (Deerfield Beach, Fla.), 27*(1), 101-108.

Wu, X., Gong, Y., Xu, S., Yan, Z., Zhang, X., & Yang, S. (2019). Electrical Conductivity of Lithium Chloride, Lithium Bromide, and Lithium Iodide Electrolytes in Methanol, Water, and Their Binary Mixtures. *Journal of Chemical & Engineering Data, 64*(10), 4319-4329. doi:10.1021/acs.jced.9b00405

Wu, X., Yang, H., Yu, M., Liu, J., & Li, S. (2021). Design principles of high-voltage aqueous supercapacitors. *Materials Today Energy, 21*, 100739.

Xu, K., Ding, M. S., & Jow, T. R. (2001). Quaternary onium salts as nonaqueous electrolytes for electrochemical capacitors. *Journal of the Electrochemical Society, 148*(3), A267.

Xu, Q., Schwandt, C., Chen, G. Z., & Fray, D. J. (2002). Electrochemical investigation of lithium intercalation into graphite from molten lithium chloride. *Journal of Electroanalytical Chemistry, 530*(1), 16-22. doi:https://doi.org/10.1016/S0022-0728(02)00998-1

Yang, J., Bissett, M. A., & Dryfe, R. A. (2021). Investigation of Voltage Range and Self-Discharge in Aqueous Zinc-Ion Hybrid Supercapacitors. *ChemSusChem, 14*(7), 1700-1709.

Yin, J., Zheng, C., Qi, L., & Wang, H. (2011). Concentrated NaClO4 aqueous solutions as promising electrolytes for electric double-layer capacitors. *Journal of Power Sources, 196*(8), 4080-4087. doi:https://doi.org/10.1016/j.jpowsour.2010.12.064

Zhang, K., Sun, J., Lei, E., Ma, C., Luo, S., Wu, Z., . . . Liu, S. (2022). Effects of the pore structure of commercial activated carbon on the electrochemical performance of supercapacitors. *Journal of Energy Storage, 45*, 103457.

Zhang, Q.-G., Sun, S.-S., Pitula, S., Liu, Q.-S., Welz-Biermann, U., & Zhang, J.-J. (2011). Electrical Conductivity of Solutions of Ionic Liquids with Methanol, Ethanol, Acetonitrile, and Propylene Carbonate. *Journal of Chemical & Engineering Data, 56*(12), 4659-4664. doi:10.1021/je200616t

Zhang, Y., Lewis, N. H. C., Mars, J., Wan, G., Weadock, N. J., Takacs, C. J., . . . Maginn, E. J. (2021). Water-in-Salt LiTFSI Aqueous Electrolytes. 1. Liquid Structure from Combined Molecular Dynamics Simulation and Experimental Studies. *The Journal of Physical Chemistry B, 125*(17), 4501-4513. doi:10.1021/acs.jpcb.1c02189

Zhao, N., Fan, H., Zhang, M., Ma, J., Du, Z., Yan, B., . . . Jiang, X. (2020). Simple electrodeposition of MoO3 film on carbon cloth for high-performance aqueous symmetric supercapacitors. *Chemical Engineering Journal, 390*, 124477.

Zheng, J., Tan, G., Shan, P., Liu, T., Hu, J., Feng, Y., . . . Pan, F. (2018). Understanding Thermodynamic and Kinetic Contributions in Expanding the Stability Window of Aqueous Electrolytes. *Chem, 4*(12), 2872-2882. doi:https://doi.org/10.1016/j.chempr.2018.09.004

# APPENDIX

# APPENDIX A
# SUPPLEMENTATION DATA

**Table A.1** The comparison electrochemical parameter of LiCl, LiBr, LiI, $LiNO_3$, $Li_2SO_4$ and LiTFSI electrolytes from different concentrations using AC-coated electrode as a working electrode.

| Electrolytes | Concentration *m* (mol/kg) | Potential window* (V) | Specific capacitance (F/g) |
|---|---|---|---|
| **LiCl** | 1 | 2.06 | 27.92 |
| | 5 | 2.22 | 32.37 |
| | 10 | 2.22 | 11.19 |
| | 15 | 2.28 | 39.69 |
| | 20 | 2.25 | 6.34 |
| **LiBr** | 1 | 2.14 | 27.11 |
| | 5 | 1.91 | 44.94 |
| | 10 | 1.92 | 47.87 |
| | 15 | 1.80 | 45.83 |
| **LiI** | 1 | 1.57 | 62.16 |
| | 5 | 1.55 | 176.32 |
| | 10 | 1.28 | 86.40 |
| **$LiNO_3$** | 1 | 2.18 | 54.59 |
| | 5 | 2.25 | 57.66 |
| | 10 | 2.26 | 48.26 |
| | 15 | 2.23 | 59.36 |
| | 20 | 2.29 | 38.87 |
| **$Li_2SO_4$** | 1 | 1.33 | 21.65 |
| | 2 | 1.38 | 26.49 |
| | 3 | 1.30 | 24.78 |
| **LiTSFI** | 1 | 1.79 | 29.20 |
| | 5 | 1.94 | 35.97 |
| | 10 | 2.05 | 45.16 |
| | 15 | 2.26 | 49.96 |
| | 20 | 2.44 | 50.31 |

* The potential window was evaluated from CV curve at a scan rate of 100 $mV.s^{-1}$.

**Table A.2** The comparison electrochemical parameter of LiCl, LiBr, LiI, $LiNO_3$, $Li_2SO_4$ and LiTFSI electrolytes from different concentrations using activated carbon in two electrode system (coin cell).

| Electrolytes | Current density (A/g) | Potential voltage (V) | Cell capacitance (F/g) | Energy density (Wh/kg) | Power density (W/kg) |
|---|---|---|---|---|---|
| **LiCl** | 0.3 | 0.71 | 5.61 | 1.40 | 762.26 |
| | 0.2 | 0.78 | 7.47 | 2.28 | 563.18 |
| | 0.1 | 0.87 | 11.30 | 4.28 | 313.49 |
| | 0.075 | 0.90 | 13.04 | 5.25 | 242.30 |
| | 0.05 | 0.93 | 16.35 | 7.00 | 166.57 |
| **LiBr** | 0.3 | - | - | - | - |
| | 0.2 | - | - | - | - |
| | 0.1 | 0.26 | 0.23 | 0.01 | 92.99 |
| | 0.075 | 0.37 | 0.20 | 0.01 | 100.09 |
| | 0.05 | 0.51 | 0.30 | 0.04 | 91.08 |
| **LiI** | 0.3 | 0.49 | 6.83 | 0.83 | 531.14 |
| | 0.2 | 0.49 | 15.45 | 1.87 | 354.10 |
| | 0.1 | 0.76 | 16.77 | 4.81 | 272.56 |
| | 0.075 | 0.78 | 13.76 | 4.24 | 211.90 |
| | 0.05 | 0.83 | 14.16 | 4.89 | 149.65 |
| **$LiNO_3$** | 0.3 | 0.88 | 44.37 | 17.19 | 950.72 |
| | 0.2 | 0.92 | 45.44 | 19.26 | 662.90 |
| | 0.1 | 0.96 | 46.84 | 21.63 | 346.00 |
| | 0.075 | 0.97 | 47.27 | 22.30 | 262.25 |
| | 0.05 | 0.98 | 48.13 | 23.19 | 176.71 |
| **$Li_2SO_4$** | 0.3 | 0.89 | 18.44 | 7.33 | 962.60 |
| | 0.2 | 0.92 | 21.47 | 9.17 | 665.35 |
| | 0.1 | 0.96 | 26.56 | 12.30 | 346.43 |
| | 0.075 | 0.97 | 28.37 | 13.42 | 262.66 |
| | 0.05 | 0.98 | 30.95 | 14.92 | 176.76 |
| **LiTSFI** | 0.3 | 0.80 | 28.59 | 9.14 | 863.68 |
| | 0.2 | 0.87 | 32.14 | 12.06 | 623.74 |
| | 0.1 | 0.93 | 37.29 | 16.26 | 336.17 |
| | 0.075 | 0.95 | 39.02 | 17.63 | 256.66 |
| | 0.05 | 0.97 | 41.12 | 19.23 | 174.10 |

* The result was evaluated from GCD curve.

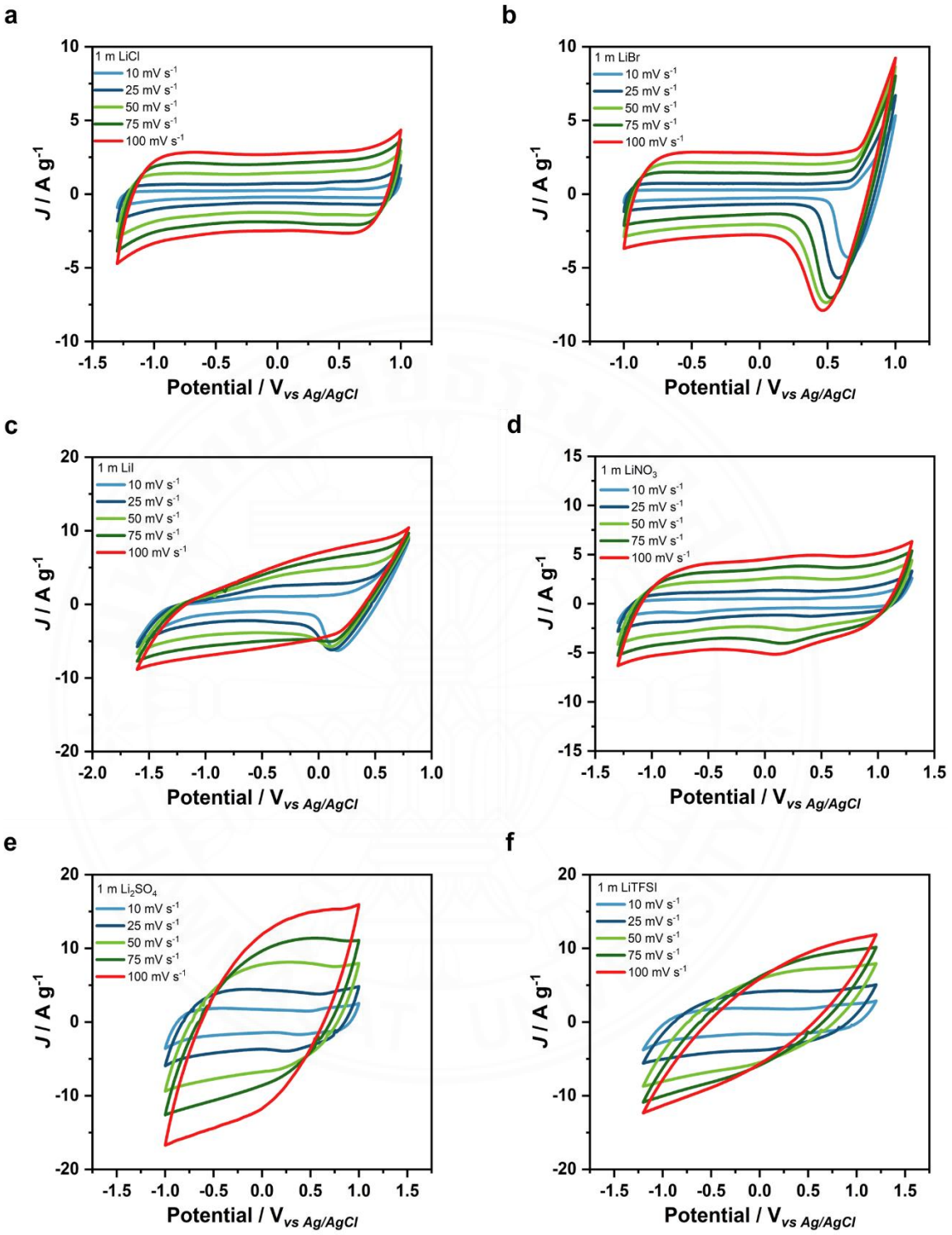


**Figure A.1** The CV response of AC-coated on glassy carbon electrode at a variety of scan rates with low and high concentrations e.g. (a) 1m LiCl, (b) 1 m Libr, (c) 1 m LiI, (d) 20 m $LiNO_3$, (e) 1m $Li_2SO_4$, and (f) 1 m LiTFSI.

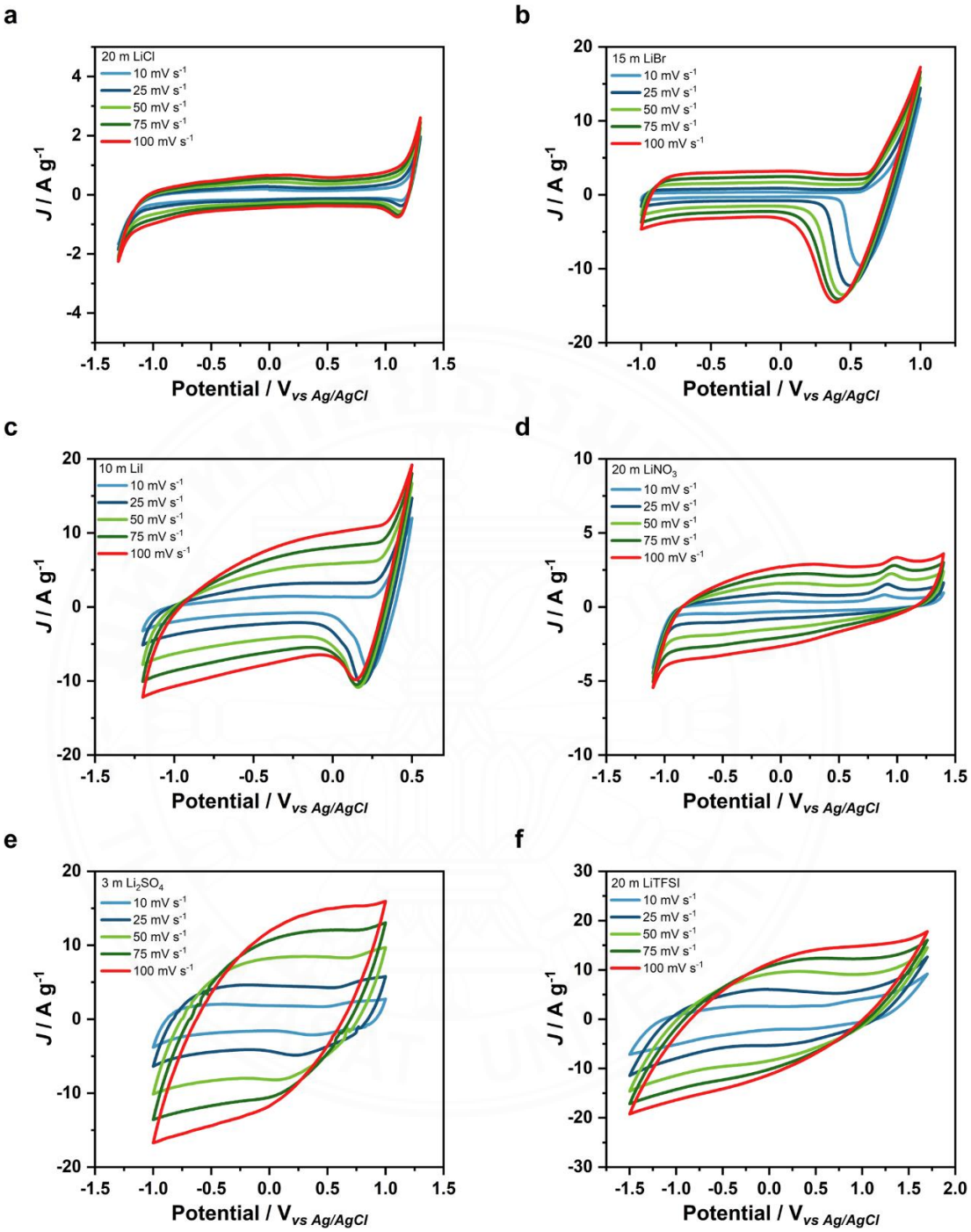


**Figure A.2** The CV response of AC-coated on glassy carbon electrode at a variety of scan rates with low and high concentrations e.g. (a) 20 m LiCl, (b) 15 m LiBr, (c) 10 m LiI, (d) 20 m $LiNO_3$, (e) 3 m $Li_2SO_4$, and (f) 20 m LiTFSI.

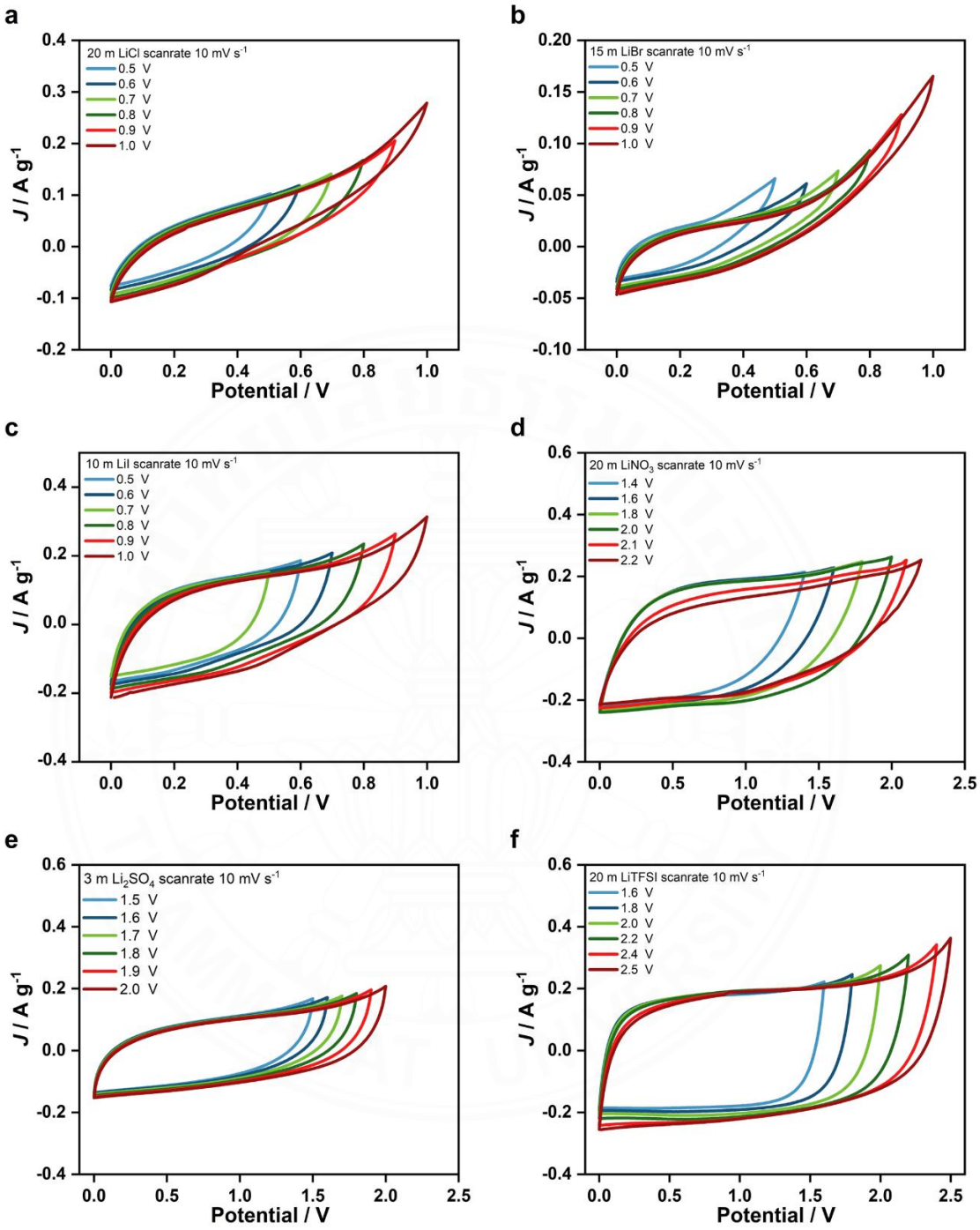


**Figure A.3** The CV response of two electrode system (coin cell) at a variety of potential voltage with high concentration eg. (a) 20 m LiCl, (b) 15 m LiBr, (c) 10m LiI (d) 20 m $LiNO_3$, (e) 3 m $Li_2SO_4$, and (f) 20 m LiTFSI.

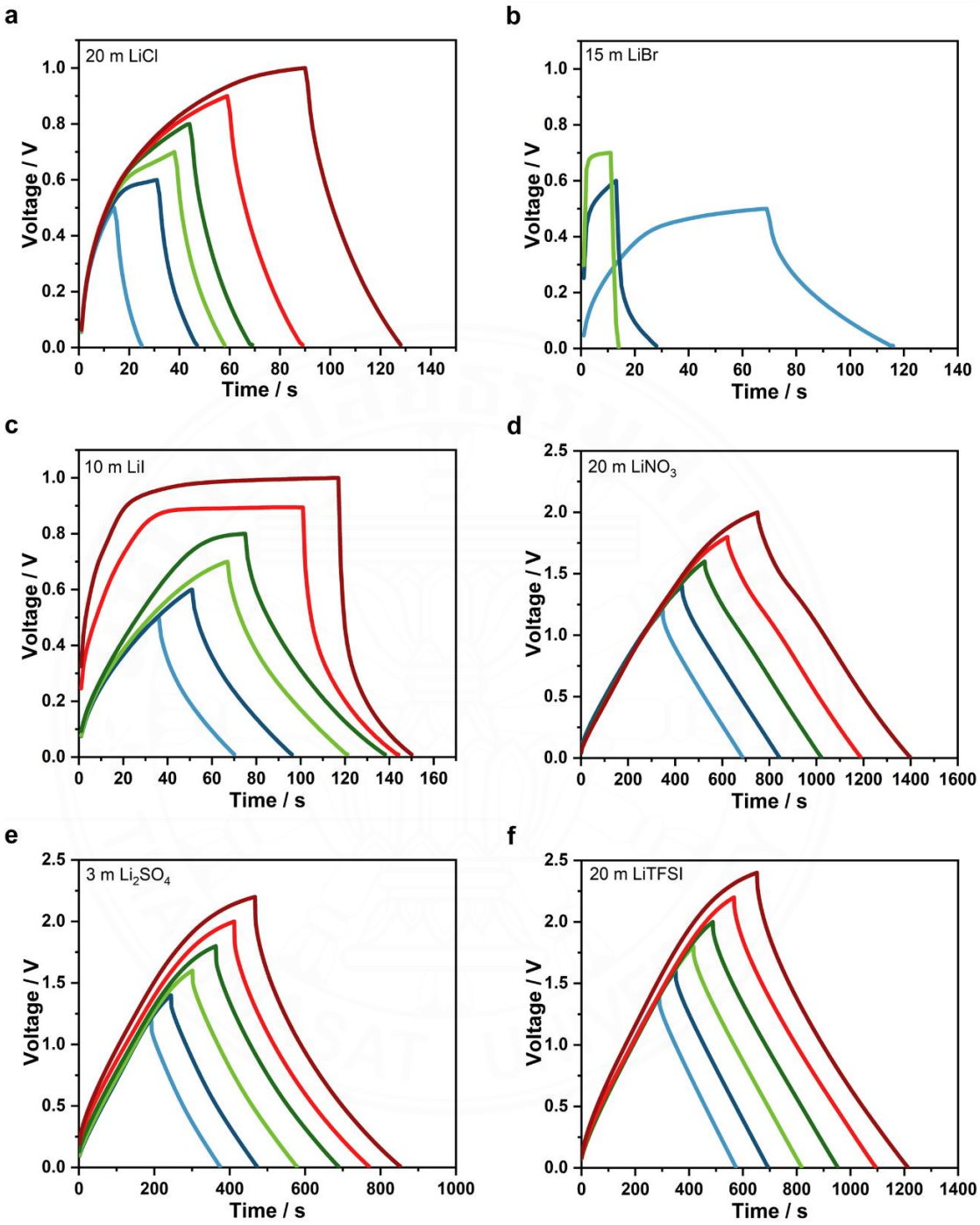


**Figure A.4** The GCD responses of two electrode system (coin cell) at a variety of potential voltage with high concentration eg. (a) 20 m LiCl, (b) 15 m LiBr, (c) 10m LiI (d) 20 m $LiNO_3$, (e) 3 m $Li_2SO_4$, and (f) 20 m LiTFSI.

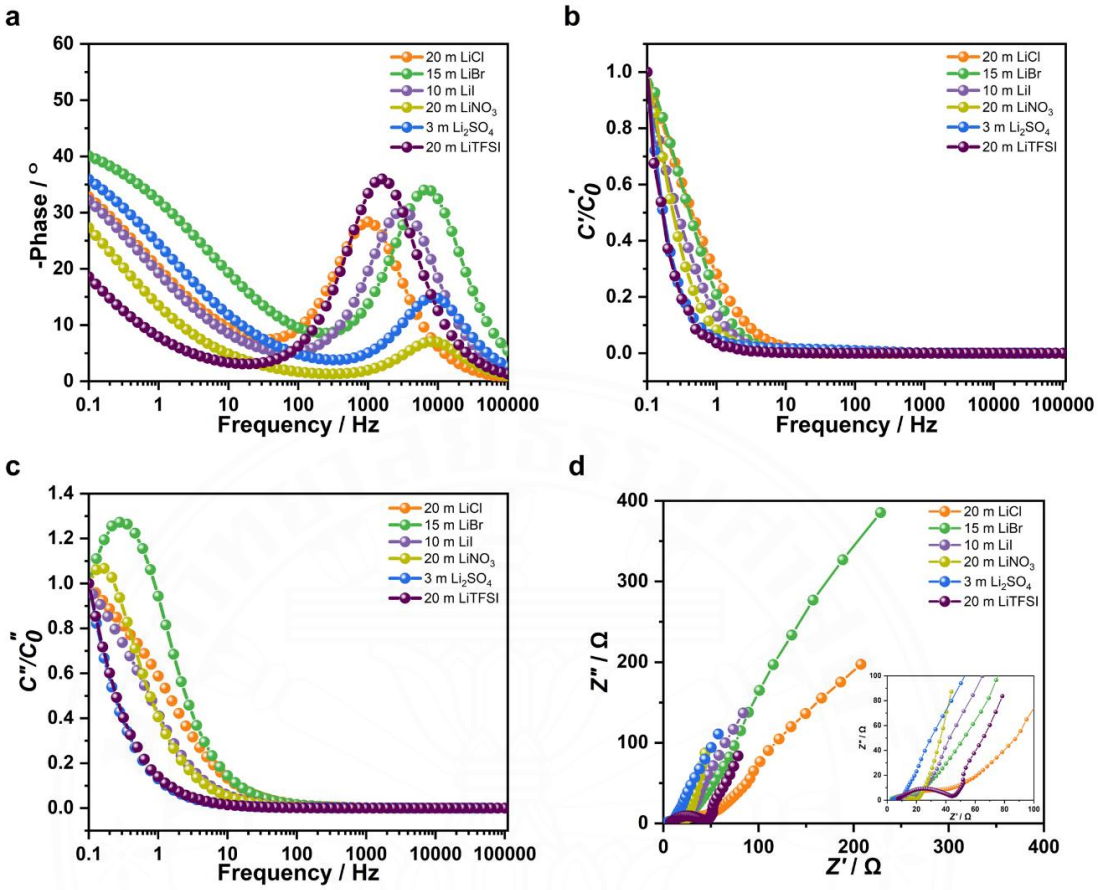


**Figure A.5** Plot of (a) phase angle against frequency (Bode plot), (b) normalized real capacitance, (c) normalised imaginary capacitance, and (d) Nyquist plots of difference electrolytes for a various electrolyte at superconcentration in two electrode system (coin cell).

# BIOGRAPHY

| | |
|---|---|
| Name | Aritsa Bunpheng |
| Education | 2018: Bachelor of Science (Chemistry)<br>Faculty of Science<br>Kasetsart University, Thailand |

Publications

Bunpheng, A., Sakulaue, P., Hirunpinyopas, W., Nueangnoraj, K., Luanwuthi, S., & Iamprasertkun, P. (2023). Revisiting the properties of lithium chloride as "water-in-salt" electrolyte for pouch cell electrochemical capacitors. *Journal of Electroanalytical Chemistry*, *944*, 117645.

Bunpheng, A., Chavalekvirat, P., Tangthana-umrung, K., Deerattrakul, V., Nueangnoraj, K., Hirunpinyopas, W., & Iamprasertkun, P. (2025). A comprehensive study of affordable "water-in-salt" electrolytes and their properties. *Green Chemical Engineering*, 6(1), 126-135.